AD_____

Award Number: W81XWH-06-1-0432

TITLE: A New In Vitro Model of Breast Cancer Metastasis to Bone

PRINCIPAL INVESTIGATOR: Andrea M. Mastro, Ph.D.

CONTRACTING ORGANIZATION: Pennsylvania State University
University Park, PA 16802

REPORT DATE: April 2008

TYPE OF REPORT: Annual

PREPARED FOR: U.S. Army Medical Research and Materiel Command
Fort Detrick, Maryland 21702-5012

REPORT DOCUMENTATION PAGE

Form Approved
OMB No. 0704-0188

1. REPORT DATE	2. REPORT TYPE	3. DATES COVERED
14-04-2008	Annual	15 MAR 2007 - 14 MAR 2008

4. TITLE AND SUBTITLE
A New In Vitro Model of Breast Cancer Metastasis to Bone

5a. CONTRACT NUMBER

5b. GRANT NUMBER
W81XWH-06-1-0432

5c. PROGRAM ELEMENT NUMBER

6. AUTHOR(S)
Andrea M. Mastro, Ph.D.

Email: a36@psu.edu

5d. PROJECT NUMBER

5e. TASK NUMBER

5f. WORK UNIT NUMBER

7. PERFORMING ORGANIZATION NAME(S) AND ADDRESS(ES)

The Pennsylvania State University
University Park, PA 16802

8. PERFORMING ORGANIZATION REPORT NUMBER

9. SPONSORING / MONITORING AGENCY NAME(S) AND ADDRESS(ES)
U.S. Army Medical Research and Materiel Command
Fort Detrick, Maryland 21702-5012

10. SPONSOR/MONITOR'S ACRONYM(S)

11. SPONSOR/MONITOR'S REPORT NUMBER(S)

12. DISTRIBUTION / AVAILABILITY STATEMENT
Approved for Public Release; Distribution Unlimited

13. SUPPLEMENTARY NOTES

14. ABSTRACT

The use of a bioreactor system has permitted the growth of osteoblasts lines and primary osteoblasts into osteoid, bone-like tissue. Over the course of months in culture, pre-osteoblasts matured to osteoblasts and eventually to osteocyte-like cells. This is the first system, that we are aware of, that permits this full range of osteogenesis. The system supports the growth of primary osteoblasts as well as osteoblast lines. The addition of breast cancer cells to the cultures, brought about profound effects on the osteoid tissue. The osteoblasts changed from cuboidal to spindle shaped and were less adherent to the substrate. The cancer cells aligned themselves with the osteoblasts into an "Indian filing" pattern. The breast cancer also penetrated the osteoid tissue. Extracellular matrix was degraded. These interactions of breast cancer cells with osteoblasts in vitro have not been previously detected. With both the primary osteoblasts and the MC3T3-E1 cell line, the cancer cells inhibited osteoblast gene expression of osteoblast differentiation proteins, but stimulated production of inflammatory cytokines. Microarray data of osteoblasts treated with growth medium versus conditioned medium from MDA-MB231 breast cancer cells supported the switch in pattern from differentiation to inflammation. In addition the microarray data indicated that several adhesion molecules were down regulated. Taken together, these data suggest that the osteoblasts in the bioreactor mimic those in metaphyseal areas of bone. The system should be useful as an *in vivo* surrogate.

15. SUBJECT TERMS

None listed.

16. SECURITY CLASSIFICATION OF:			17. LIMITATION OF ABSTRACT	18. NUMBER OF PAGES	19a. NAME OF RESPONSIBLE PERSON
a. REPORT	b. ABSTRACT	c. THIS PAGE			USAMRMC
U	U	U	UU	78	19b. TELEPHONE NUMBER *(include area code)*

Table of Contents

Page

Progress Report: A New In Vitro Model of Breast Cancer Metastasis to Bone

Andrea M. Mastro, Carol V. Gay and Erwin A. Vogler

INTRODUCTION:

Breast cancer frequently metastasizes to the bone where it disrupts the balance of osteoblasts and osteoclasts and leads to osteolytic degradation (Bussard et al. 2008). The objective of this study was to test the hypothesis that osteolytic bone metastases results partly from the affect of the cancer cells on the osteoblasts, i.e. the cancer cells prevent osteoblasts from accreting mineralized tissue ultimately leading to accelerated skeletal degradation. In order to test this idea, we proposed to develop an existing three-dimensional culture system into an *in vitro* test system for studying the interactions between osteoblasts and metastatic breast cancer cells. The objectives were to characterize the morphology and physiology of osteoblasts (MC3T3-E1) cultured as a 3D osteoid in a bioreactor and to determine how they reacted to the presence of human metastatic breast cancer cells (MDA-MB-231).

BODY:

***Task 1*. To determine the effects of metastatic breast cancer cells on the physiology of osteoblasts cultured in a long term culture system that fosters growth in three-dimensions. (months 1-6)**

a. Establish cultures of MC3T3-E1 cells in bioreactors and add metastatic breast cancer cells at various times after the establishment of culture (4,7,15,30 days). Periodically sample the secreted materials in the growth chamber that will indicate osteoblast function. ELISA or RIA will be carried out for OCN, IL-6, MIP-2, MCP-1. Alkaline phosphatase will be assayed by a biochemical assay. Culture medium from cells grown in standard tissue culture will be compared. For control cells in selected assays, a human immortalized non-tumorgenic cell line, such as h-TERT–HME1 will be used.

b. Establish cultures of MC3T3-E1 cells in bioreactors and add metastatic breast cancer cells at various times after the establishment of culture bioreactors as in task 1-a. Terminate the cultures periodically to assay the cells for cell associated alkaline phosphatase, Type I collagen, mineralization (alizarin red, von Kossa) and for apoptosis (TUNEL).

***Task 2*. To determine the effects of metastatic breast cancer cells on osteoblast morphology in a long term bioreactor culture system that fosters growth in 3-dimensions. (months 7-13)**

a. Co –cultures of osteoblasts and breast cancer cells will be prepared as in task 1. The stage of differentiation of the osteoblasts and the time of the addition of the cancer cells will be decided based on the results of task 1. Co-cultures from the bioreactor and conventional cultures will be fixed to preserve morphological detail.

b. Part of each culture will be fixed with paraformaldehyde following a protocol to preserve GFP. These cultures will be imaged with confocal fluorescence microscopy to detect the metastatic breast cancer cell migration.

c. Part of each culture will be prepared for detection of apoptosis (TUNEL). The GFP tag of the cancer cells will allow us to distinguish apoptotic cancer cells from apoptotic osteoblasts.

d. Part of each culture will be prepared for scanning electron microscopic observation. We anticipate that we will be able to distinguish cancer cells from osteoblasts in these preparations based on size and shape.

e. Part of each culture will be prepared for the transmission electron microscopy. We will view the cells with an eye to fine structural detail.

Summary of the results of the Second Year of Investigation

Parts of tasks 1 and 2 were pursued in parallel to maximize efficiency in achieving aims of proposed work and to provide internal consistency in the work by using living cells/biological materials in a conserved timeframe. Much of aim 1 was reported last year.

1. Task 1: Characterization of osteoblasts in the bioreactor:

Main finding: Osteoblast lines and as well as primary osteoblasts grow into bone osteoid-like tissue in the bioreactor. They express characteristic differentiation genes and osteoblast-secreted molecules and cytokines.

In last year's report we presented a publication and data to show that osteoblast lines grow into multi-cell layers in the specialized bioreactor (Dhurjati et al. 2006). In the meantime, we also published a study describing the characterization of the fundamental properties of the substratum used in the bioreactor and how the various conditions affected osteoblast growth (Liu et al. 2007). In brief, osteoblasts attached and grew on both hydrophilic surfaces (plasma treated quartz, plasma treated glass, tissue-culture grade polystyrene) and hydrophobic surfaces (bacterial grade polystyrene, silane-treated quartz). However the attachment process was delayed on the hydrophobic surfaces (Liu et al. 2007, Figures 3 and 4). This delay was apparent from the morphology (Figure 5), and from the expression of adhesion molecules (Figure 8). For extended growth of osteoblasts in the specialized bioreactor, we chose gas-permeable films of Suryln 1702 resin (Dhurjati et al. 2006).

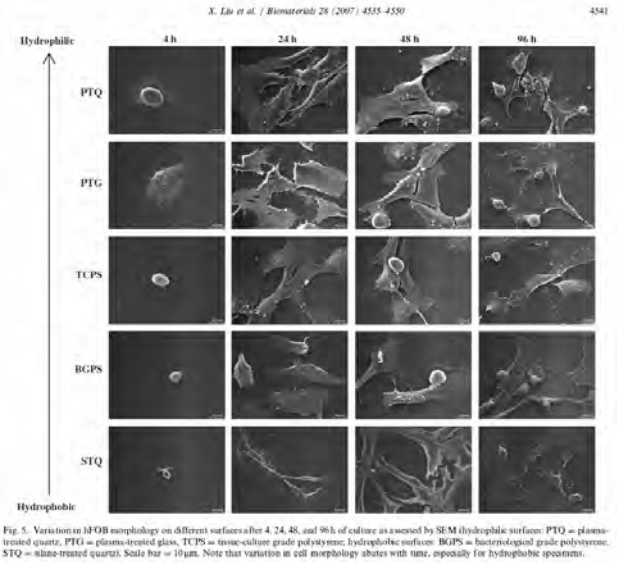

Fig. 5. Variation in hFOB morphology on different surfaces after 4, 24, 48, and 96 h of culture as assessed by SEM (hydrophilic surfaces: PTQ = plasma-treated quartz, PTG = plasma-treated glass, TCPS = tissue-culture grade polystyrene; hydrophobic surfaces: BGPS = bacteriological grade polystyrene, STQ = silane-treated quartz). Scale bar = 10 μm. Note that variation in cell morphology abates with time, especially for hydrophobic specimens.

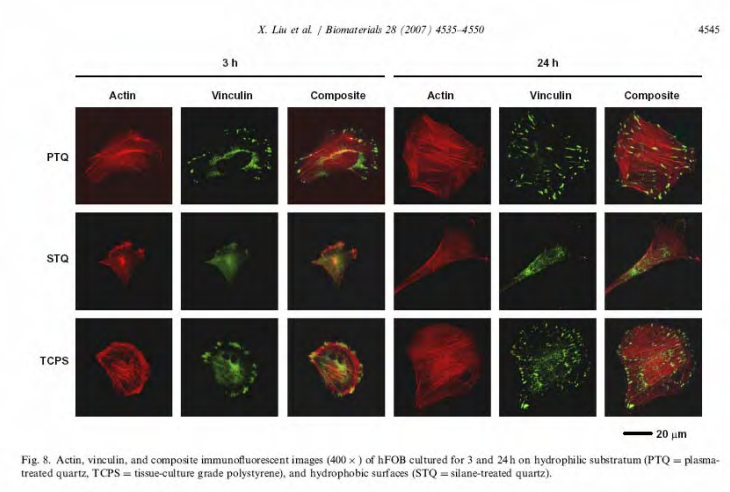

Fig. 8. Actin, vinculin, and composite immunofluorescent images (400 ×) of hFOB cultured for 3 and 24 h on hydrophilic substratum (PTQ = plasma-treated quartz, TCPS = tissue-culture grade polystyrene), and hydrophobic surfaces (STQ = silane-treated quartz).

Figure 1 (left), comparison of osteoblast morphology over time when plated on hydrophilic and hydrophobic surfaces.

Figure 2 (right), expression of vinculin by osteoblasts after 3 or 24 hr. culture on hydrophobic (saline treated quartz), tissue culture grade polystyrene (TGPS) or hydrophilic surface (plasma treated quartz). We also determined the expression of osteoblast differentiation molecules in osteoblasts grown in the bioreactor over extended periods of time (Figure 2 Dhurjati et al. submitted manuscript, appendix) and Figure 4 (Shuman et al. submitted manuscript, appendix).

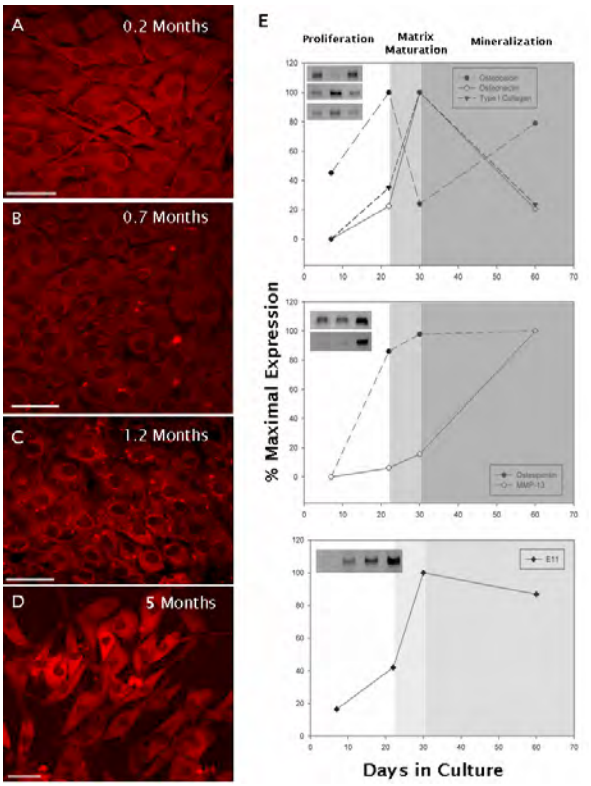

Figure 3. Maturation of MC3T3-E1 derived osteoid tissue with the bioreactor. Panels A-D are confocal images of actin-stained cells over several months of continuous culture (scale bar = 50 μm). Spindle-shaped pre-osteoblast (A) progressively transformed into cuboidal osteoblasts (B) that became enmeshed in a collagenous matrix, that appears black in the image (C), that eventually buried the cells which exhibited an osteocyte-like morphology. (see Dhurjati et al. submitted.) As the cells mature, they express characteristic molecules of differentiation as determined by RT-PCR (Panel E).

Figure 4. Expression of osteoblast differentiation genes, over time in standard cell culture conditions and in the bioreactor. MC3T3-E1 cells were cultured in a bioreactor or in polystyrene culture dishes . At indicated times (22, 30, 60 days for the bioreactor samples and 5, 7, 11, and 21 days for cell culture samples) the cells were harvested and RNA isolated (RNeasy kit, Qiagen). RT-PCR was carried out . Ethidium bromide stained bands were quantified using Imagequant (Molecular Dynamics) and were normalized to β-actin. Shown are representative amplicon bands .

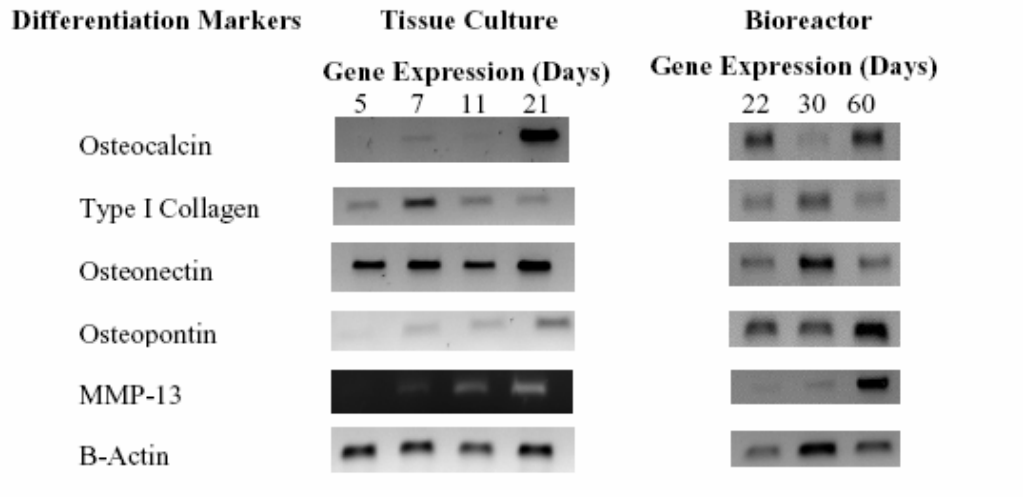

We also were able to grow primary osteoblast in the bioreactor system. Osteoblasts were isolated from the calvariae of 2 day-old FVBN, Smad3 heterozygous pups. Cells were inoculated into a bioreactor and allowed to remain for 90 days. The cultures were monitored microscopically every few days. Before dismantling the chamber, the cells were stained with Cell Tracker Orange ™ and imaged by confocal microscopy. At the end of the incubation, cells were stained for alkaline phosphatase or with the von kossa procedure to examine osteoblast maturation and mineralization. The primary cells in the bioreactor formed multilayers and looked healthy (Figure 5). They were positive for mineralization as indicated by the von kossa stain. RNA was extracted from the cells; we are in the process of testing it by RT-PCR for the expression of osteoblast differentiation genes.

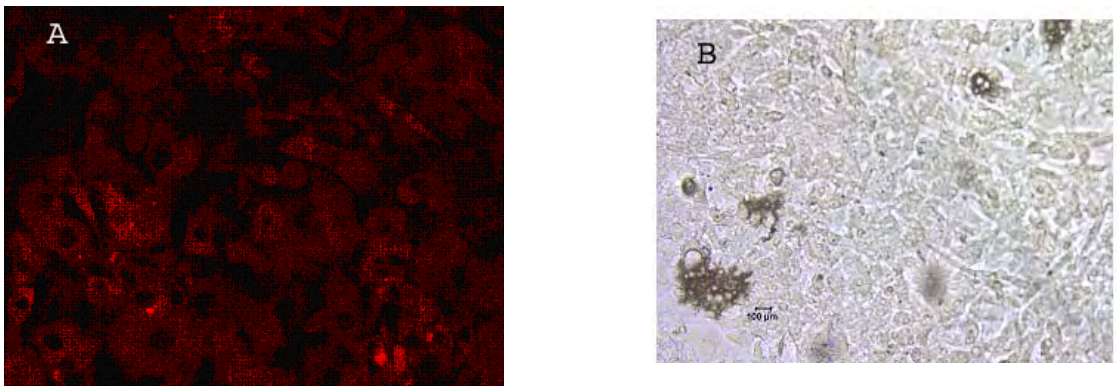

Figure 5. Primary osteoblasts grown for 90 days in the bioreactor. Calvarial osteoblasts from 2 day FVBN pups were inoculated into a bioreactor; after 90 days the cells were stained with Cell Tracker Orange ™ and visualized by confocal microscopy (A). Sections were also stained by von kossa for mineralization (B).

Significance: Osteoblasts, both lines and primary cells, in the bioreactor grow into an osteoid tissue. The cells express characteristic osteoblast differentiation molecules. Moreover, they produce an extracellular matrix that is prone to mineralization. Over time, i.e. 10 months, the cells take on the appearance of osteocytes. This is the only reported culture system for growing osteocytes that we are aware of. The growth of the primary cultures will allow us to isolate osteoblasts from mice with mutations or transgenics with knockouts in selected osteoblast molecules, e.g. PTHrP.

Task 2. To determine the effects of metastatic breast cancer cells on osteoblast morphology in a long-term bioreactor culture system that fosters growth in 3-dimension.

Main findings: Culture of metastatic breast cancer cells with osteoblasts grown as a three dimensional tissue, revealed an osteoblast and a cancer cell response similar in many ways to that reported in pathological tissue; i.e. the cancer cells penetrated the osteoblast tissue, the osteoblast changed morphology, expressed inflammatory cytokines and turned off expression of genes related to differentiation. The cancer cells aligned themselves with the osteoblasts in a pattern characteristic of "Indian filing."

We reported last year that metastatic breast cancer cells (MDA-MB-231) grew in the bioreactor, penetrated the bone-like matrix, and caused the osteoblasts to undergo a change in morphology from cuboidal to elongated. We have repeated that experiment several times. The results are contained in the appended manuscript (Dhurarti et al. submitted).

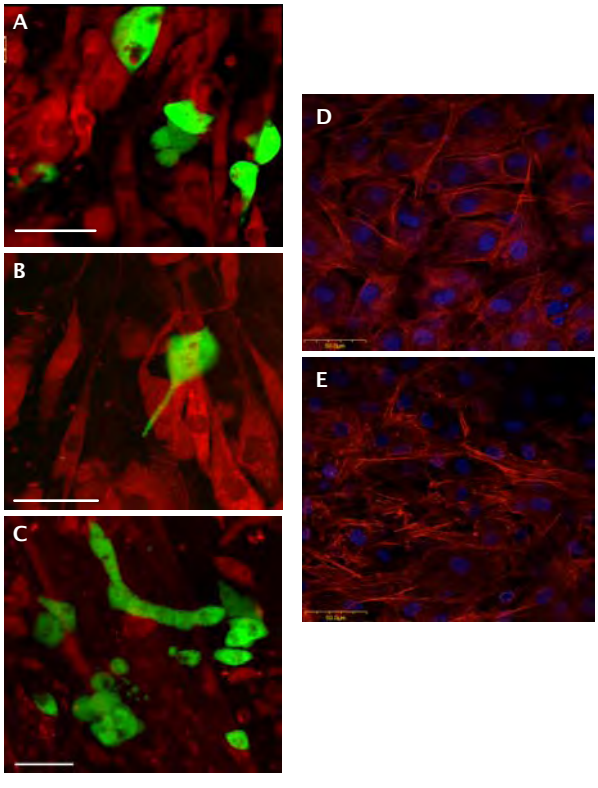

Figure 6. MDA-MB-231^{GFP} invasion of MC3T3-E1 derived osteoid tissue (OT) grown for 5 months within the bioreactor. Osteoblasts, stained with Cell Tracker Orange™ were cultured with MDA-MB-231$^{GFP.}$ Confocal images were collected over three days. Representative images indicate breast cancer cell adhesion (A), penetration of the osteoid tissue (B), and organization of the cancer cells into "Indian files." Panels D, E, are images of osteoblasts grown for 16 days in the bioreactor. Conditoned medium from breast cancer cells was added at day 2. The cells were stained with phalloidin for actin filaments and Draq 5 for nuclear staining. (from Dhurjati et al. submitted).

Included here are figures of breast cancer cell adherence, penetration and growth in the osteoblast layer. The cancer cells appeared to send processes into the area surrounding the cells (black on the figures). In addition the cancer cells aligned with one another in a manner reminiscent of "Indian filling." When the osteoblasts were grown in conditioned medium from the cancer cell, they exhibited a change in actin fiber arrangements. We had previously seen this change in morphology in tissue culture experiments (Mercer et al, 2004; Mercer and Mastro 2005).

The osteoblasts tissue not only lost extracellular matrix, but they produced less collagen and less osteocalcin, important for mineralization (Figure 7).

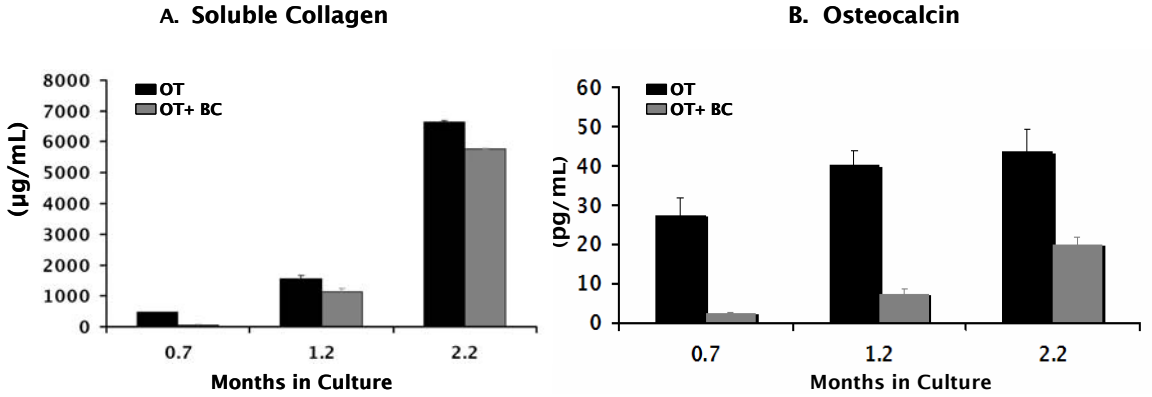

Figure 7. Co-culture of MDA-MB 231 metastatic beast cancer cells with osteoblasts caused a reduction of osteoblast collagen synthesis. Breast cancer cells were inoculated at a ratio of ~1 cancer cell to 10 osteoblasts at the times indicated. After 7 days the culture media were harvested. Soluble collagen was determined by Sircol™ and osteocalcin by a LINCOplex™ Mouse Bone Panel 2B, Millipore).

We compared co-culture of MDA-MB-231 cells with osteoblasts in co-culture and in bioreactor (Shuman et al. submitted). We found that the osteoblasts grown in a standard tissue culture plate grew mostly as monolayers of cells. We tested the addition of cancer cells to osteoblasts at ratios of 1:10, 1:100 and 1:1000 (BC:OB). The osteoblasts were in three stages of differentiation, barely confluent (day 4), mid-differentiation (day 14) and well differentiated (day 24). The cancer cells attached and grew regardless of the age of the osteoblasts or the ratio of the cancer cells (Figure 8). However, the cancer cells formed more and larger colonies on the younger osteoblasts. There was a lag in growth on the well-differentiated osteoblasts. Eventually after about two weeks, the cancer cell colonies grown on the 24 day osteoblasts reached the same size as the colonies grown for 7 days on the day 4 osteoblasts. As indicated by the percentages in the figures, the cancer cell colonies covered as much as 30% of the cultures after one or two weeks.

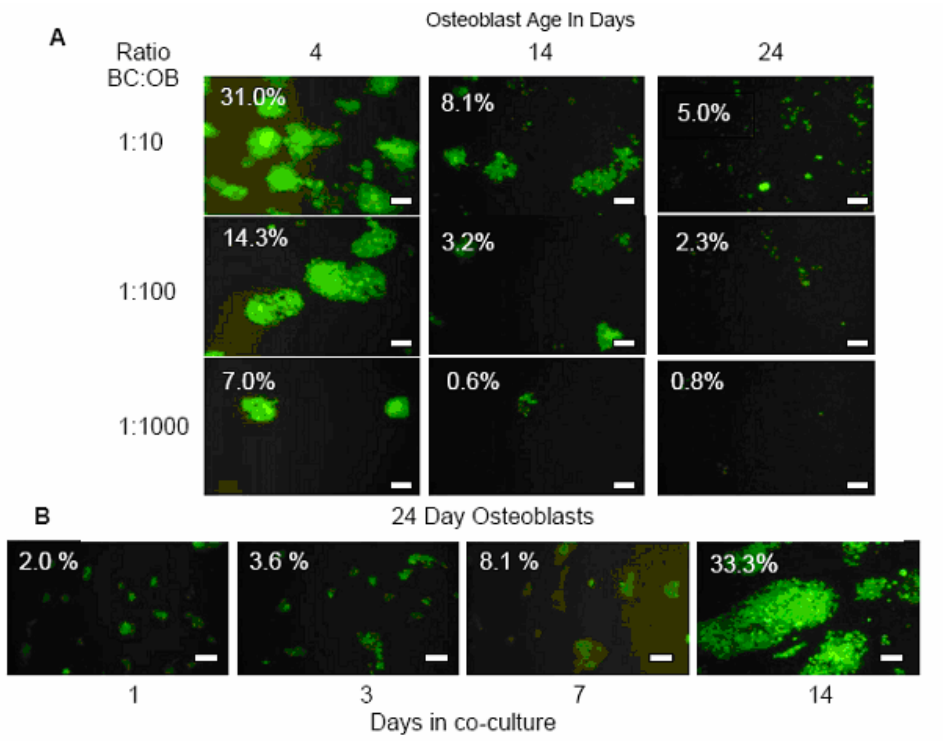

Figure 8. *Co-culture of MC3T3-E1 osteoblasts with metastatic breast cancer cells, MDA-MB-231^{-GFP}, in conventional cell culture. At various stages of osteoblast growth / differentiation (day 4, 14, or 24) breast cancer cells (BC) were added to osteoblasts (OB), at one of three ratios of BC to OB (1:10, 1:100, and 1:1000). Co-culture was carried out for 7 days. (A) The effect of increasing osteoblast differentiation state and breast cancer to osteoblast ratios on the colonization of the cultures by the cancer cells after 7 days. Shown are the fluorescence microscopic images of co-cultures. Values indicate percentage of culture area occupied by the breast cancer cells as calculated by the Image J analysis tool (NIH). Three fields were viewed and analyzed at each point (5,000X). (B) Colonization of differentiated (day 24) osteoblasts by the cancer cells at various days of co-culture up to 14 days. Breast cancer cells were added at a ratio of 1 BC:10 OB to 24-day cultures of MC3T3-E1 osteoblasts. Co-cultures were imaged after 1, 3, 7, and 14 days. Percent colonization was calculated as described in A. (from Shuman et al. submitted).*

The culture supernatant from co-cultures of breast cancer cells and osteoblasts in standard tissue culture or in the bioreactor were compared. Under both culture conditions, the presence of breast cancer cells cause on decrease in OCN and an increase in IL-6 (Figure 9). OCN is an osteoblast differentiation protein. IL-6 is one of several inflammatory molecules secreted by osteoblasts during stress.

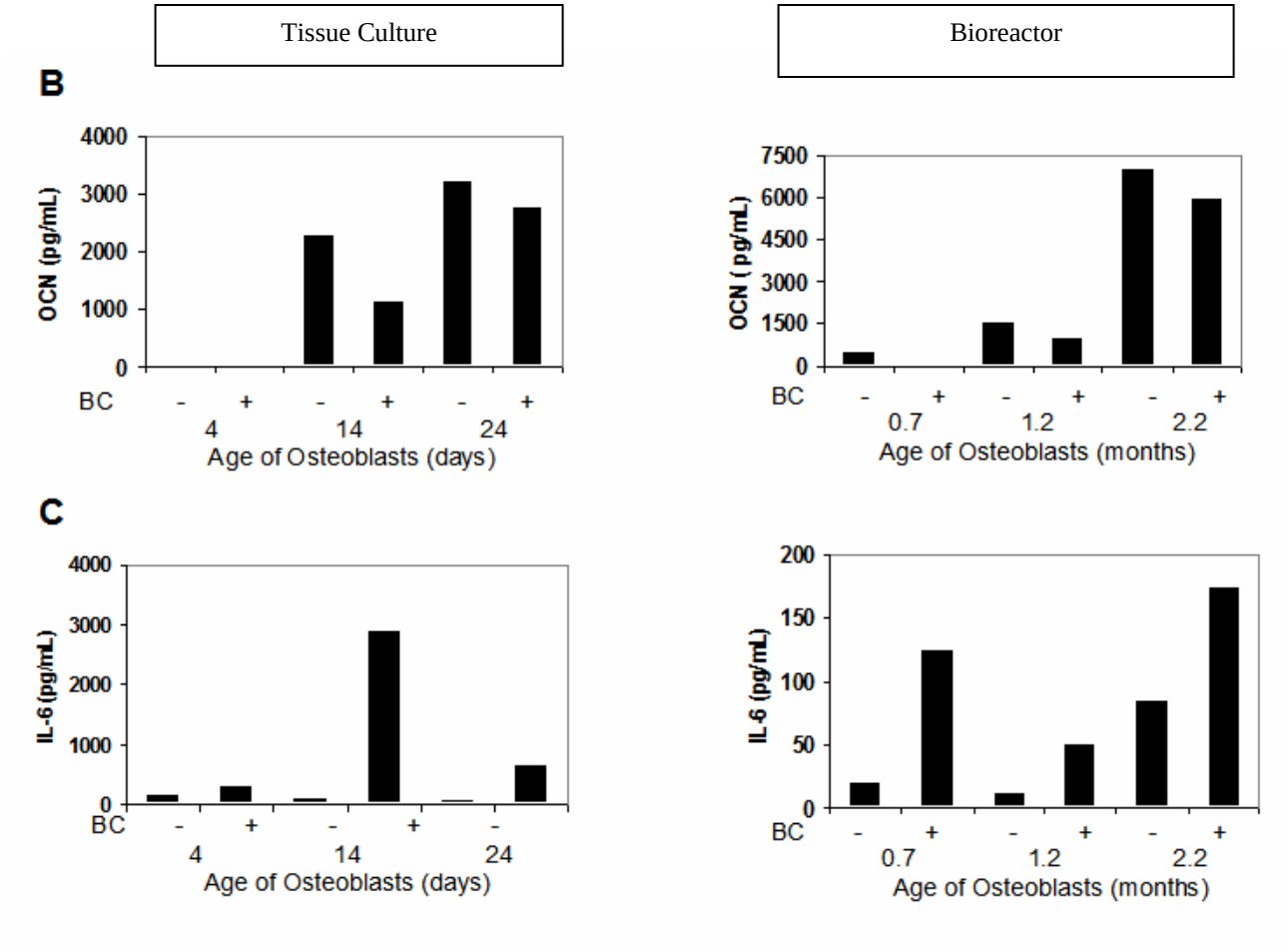

Figure 9. Quantitative plot of secreted osteocalcin protein from osteoblasts of various ages compared to osteoblasts cultured with breast cancer cells for a co-culture period of 7 days in standard cell culture (B-left) or in the bioreactor (B-right). Protein levels of the pro-inflammatory cytokine, IL-6, secreted by the osteoblasts in the presence and absence of metastatic breast cancer cells grown in standard cell culture (C-left) or in the bioreactor (C-right). IL-6 and OCN protein levels were quantitated using a mouse ELISA assay from Millipore (LINCOplex™ Mouse Bone Panel 2B).

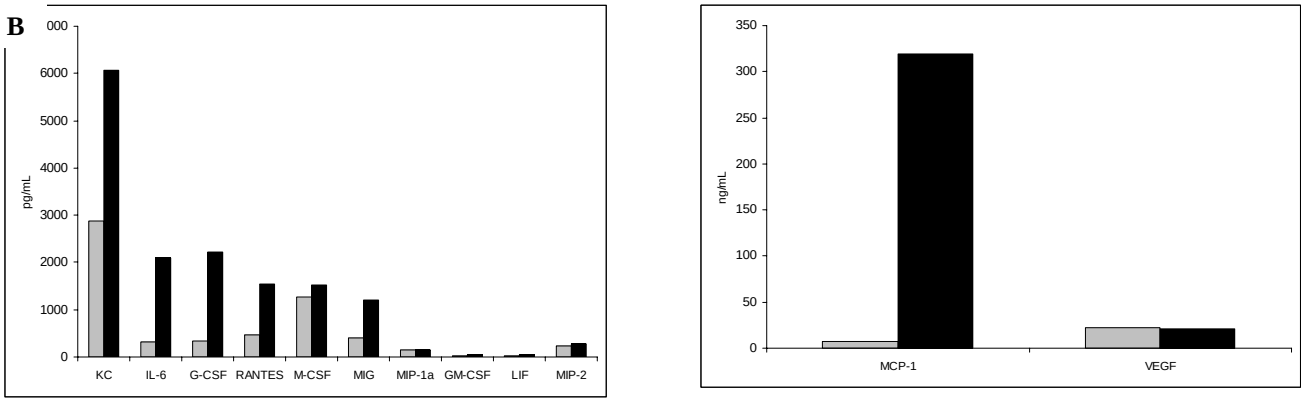

C

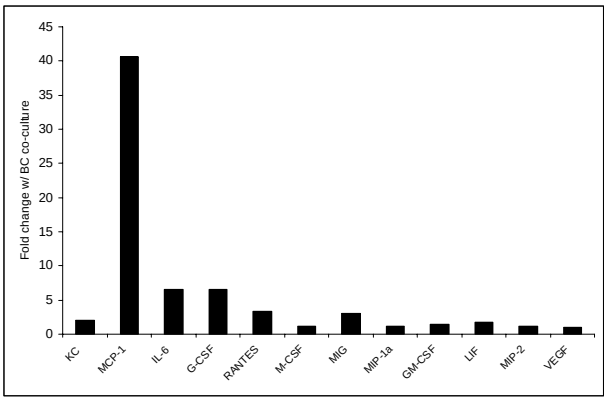

D

Cytokine levels (pg/mL)		
	OB only	**OB+BC**
KC	2,886	6,071
MCP-1	7,860	318,852
IL-6	321	2,100
G-CSF	335	2,211
RANTES	456	1,553
M-CSF	1,271	1,532
MIG	396	1,203
MIP-1a	141	156
GM-CSF	24	35
LIF	26	43
MIP-2	236	279
VEGF	21,728	21,572

Figure 10. The effect of breast cancer cells on cytokine production of MC3T3-E1 grown in the bioreactor. *MC3T3-E1 cells were grown for 60 days in the bioreactor before addition of MDA-MB-231 cells at about a 1:10 ratio of cancer cells to osteoblasts. Supernatant harvested after 7 days was assayed for the presence of the twelve cytokines indicated using a Mouse Biorad Bioplex array.*

A 12 cytokine multiplex ELISA was used to screen the supernatant from MC3T3-E1 grown for 60 days in the bioreactor and co-cultured with MDA-MB-231 cells for 7 days. The osteoblasts produced nanogram quantities of several cytokines (KC, MCP-1, M-CSF and VEGF). Others were present in smaller amounts (IL-6, G-CSF, RANTES, MIG, MIP-1a and MIP-2). Others were barely detectable (GM-CSF and LIF) (Figure 10, A,B, and D). The breast cancer cells brought about only moderate increases in most cytokines. G-CSF and IL-6 showed over six fold increases. In contrast, MCP-1 increased approximately 40 fold. Interestingly, we have found MDA-MB-231 cells produce little or no MCP-1. This cytokine plays an important role in bone remodeling. It is produced by osteoblasts and attracts and activates osteoclasts. We had previously found in tissue culture studies, that osteoblasts produced inflammatory stress response molecules, IL-6, and KC in the presence of breast cancer cells or their conditioned medium.

Microarray analyses of bioreactor cultures treated with breast cancer conditioned medium.

We compared the gene expression of osteoblasts exposed to breast cancer conditioned medium with those in normal medium. MC3T3-E1 cells grown for 15 days in the bioreactor were treated with breast cancer cell conditioned medium for 24 or 48 hours.

At the end of the time, the cells were harvested and RNA isolated. RNA samples were forwarded to the Penn State DNA Microarray Facility.

RNA sample quality was excellent as determined with an Agilent Bioanalyzer using RNA Nano Chips (Agilent, Palo Alto, CA). The arrays were manufactured by the Penn State Microarray Facility. Approximately 16,000 probes, 1 gene per probe, of the Operon (Huntsville, AL) Mouse Version 2.0 oligo set were used. Images were gridded and data were acquire and analyzed using the GenePix Pro software.

We found that the expression of approximately 239 genes were changed more than two fold after a 24 hour exposure to breast cancer conditioned medium (Table 1). Approximately 150 were similarly affected after 48 hours (Table 2). We organized the apparently most important genes into groups based on their function: adhesion and motility, osteoblast growth and differentiation, proteases, cytokines and receptors. We saw that there was a general decrease in adhesion molecules. This outcome correlated with the morphological changes, especially in osteoblast shape observed microscopically. The largest category of genes that changed was that associated with osteoblast growth and differentiation. Again, in strong correlation with data collected by other techniques, these genes are mostly down-regulated. Some, e.g. PKi gamma increased but it is a negative regulator of differentiation. Others, such as procollagen-C endopeptidase enhancer was upregulated by the TGF-Ḅ in the conditioned medium. We also saw an increase in proteases which may play a cooperative role in allowing cancer cells to migrate in the osteoid material. Cytokines such as IL-6 were still upregulated but not as sharply as seen after 4 hour exposure to conditioned medium. Stromal cell derived factor 1, a strong chemokine, was increased. Interestingly, Annexin 8, was highly (>11 fold) upregulated. Previously it has been reported to be expressed in osteoarthritis but not with normal osteoblasts. This increase may reflect osteoblasts in a stressed condition.

After 48 hours of exposure to breast cancer conditioned medium the patterns were similar to those found at 24 hours. Many genes associated with osteoblast differentiation were still downregulated. Annexin 8 was still high. Moesin, a protein associated with the cytoskeleton was upregulated. The expression of this molecule may be associated with osteoblast adhesion to the cancer cells.

Table 1. Microarray gene expression analysis of MC3T3-E1 osteoblasts cultured for 15 days in the bioreactor and treated with MDA-MB-231 breast cancer cell conditioned media for 24 hours

Gene	Fold change when treated with CM
Adhesion and motility	
Osteomodulin	-5.6
Pak3 binding protein	-5.0
Vinculin	-2.1
Matrilin	-2.1
Neural cell adhesion molecule	2.1
Osteoblast growth and differentiation	
Asporin	-3.9
Prolactin receptor	-3.9
Secreted frizzled related protein 2	-2.9
Chondromodulin	-2.6
Growth hormone receptor	-2.3
Aquaporin 1	-2.3
Insulin-like growth factor 1	-2.2
Fibroblast growth factor receptor 2	-2.2
Osteoglycin	-2.1
Peroxisome proliferative activated receptor γ	-2.1
Fibroblast growth factor 2	-2.1
CCAAT/enhancer binding protein, delta	2.2
Oncostatin receptor	2.3
Bradykinin receptor	2.7
Connective tissue growth factor	4.0
Wnt inducible signaling pathway protein 2	8.0
Proteases	
Extracellular proteinase inhibitor, WDNM1	-2.4
Tissue inhibitor of metalloproteinase 4	-2.4
Metallothionein 4	2.0
Urokinase plasminogen activator receptor	2.6
Tissue inhibitor of metalloproteinase 1	2.9
Cytokines and receptors	
IL-24	-3.3
IL-6	2.3
IL-4	2.5
IL-4 receptor	2.6
Miscellaneous	
Parathyroid hormone	2.5
Caspase 11	2.6
Hyaluronan synthase 2	2.9
Jun oncogene	3.0
Stromal cell derived factor 1	4.2
Annexin 8	11.5

Table 2. Microarray gene expression analysis of MC3T3-E1 osteoblasts culutred for 15 days in the bioreactor and treated with MDA-MB-231 breast cancer cell conditioned media for 48 hours.

Gene	Fold change when treated with CM
Adhesion and motility	
N-cadherin	-2.0
Moesin	11.2
Osteoblast growth and differentiation	
Extracellular matrix protein 1	2.0
Protein kinase inhibitor gamma	2.1
Osteomodulin	2.1
Transforming growth factor beta	2.2
Bone morphogenetic protein 10	2.4
Procollagen, type 3	2.5
Connective tissue growth factor	3.2
Wnt indcuble signaling pathway protein 2	4.8
Wnt inhibitory factor 1	5.1
procollagen-C endopeptidase enhancer	8.1
Proteases	
Extracellular proteinase inhibitor, WDNM1	-3.9
Tissue inhibitor of metalloproteinase 1	2.1
Metallothionein 4	2.7
Cytokines and receptors	
MCP-1	-5.1
CXCL-5	-2.7
IL-24	3.1
Miscellaneous	
Jun oncogene	2.2
Toll-like receptor 7	3.6
Annexin 8	7.4

Significance:

The interaction of metastatic breast cancer cells with osteoblasts in a three-dimensional culture system provides an excellent model in which to study cell-cell interaction and the bone- tumor microenvironment. The presence of the breast cancer cells causes a change in the gene-expression profile of the osteoblasts. Characteristic osteoblast differentiation proteins were downregulated. There was an increase in inflammatory cytokines and cytokines that attract osteoclasts.

***Task 3*. To test known stimulators and/or protectors of osteoblast function in the presence and absence of breast cancer cells in order to develop a means of blocking the destructive effects of breast cancer cells have on bone forming osteoblasts. (months 14-34)**

a. Establish cultures of osteoblasts at various stages of differentiation in the presence and absence of metastatic breast cancer cells as determined from task 1. Neutralizing antibodies to TGF-beta will be added and the cultures followed as in task 1.

b. Establish cultures of osteoblasts at various stages of differentiation in the presence and absence of metastatic breast cancer cells as determined from task 1. Glutamine will be added and the cultures followed as in task 1.

c. Establish cultures of osteoblasts at various stages of differentiation in the presence and absence of metastatic breast cancer cells as determined from task 1. Selenium will be increased or reduced (by used of selenium depleted serum) and the cultures will be followed as described in task 1.

d. Depending on the outcomes of a-c, combinations of these compounds will be added to the cultures. Osteoblasts will be assayed as described in Task 1.

The experiments described in task 3 have not yet been carried out in the 3-dimensional system. We have examined some of the variables in standard tissue culture in order to determine doses etc. For examples, we have grown the MC3T3-E1 osteoblasts in serum depleted medium (< 0.025 μm) and found them still capable of proliferating and differentiating (data not shown). We have previously reported that TGF-beta will block osteoblast differentiation and that addition of neutralizing antibody to the conditioned medium will prevent this effect (Mercer et al. Exp and Clin Met 2004).
These results will allow us to now test these reagents in the bioreactor systems.

Key Research Accomplishments:

- Primary osteoblasts and the MC3T3-E1 osteoblast line can be grown for extended periods in the bioreactor.
- The osteoblasts appeared to differentiate and undergo an osteogenesis program from pre-osteoblasts to mature osteoblasts to osteocytes. Gene expression and morphology indicated this progression.
- MDA-MB-231 metastatic breast cancer cells were successfully co-cultured with the osteoblasts. They caused a change in morphology of the osteoblasts. The cancer cells aligned themselves in a manner reminiscent of “Indian Filing.”
- The colonization of the breast cancer cells with osteoblasts varied with the stage of maturation of the osteoblasts.

- With both the primary osteoblasts and the MC3T3-E1 cell line, the cancer cells inhibited osteoblast differentiation genes. On the other hand they stimulated expression of inflammatory cytokines.
- Microarray data supported the change in pattern from differentiation to inflammation. In addition the microarray data indicated that several adhesion molecules were down regulated and proteases were upregulated.

REPORTABLE OUTCOMES

Manuscripts:

Liu, X., J.Y. Lim, H.J. Donahue, R. Dhurjati, A.M. Mastro, E.A. Vogler. Influence of substratum surface chemistry / energy and topography of the human fetal osteoblastic cell line. 2007. Biomaterials. hFOB1.19: phenotypic and genotypic responses observed in *in vitro*. 28:4535-4550.

Kinder M, E. Chislock, K.M. Bussard, L. Shuman, and A. M. Mastro. Metastatic breast cancer induces an osteoblast inflammatory response. 2008. Experimental Cell Research. 314 173-189.

Bussard, K.M.,C. V. Gay, A. M. Mastro. The bone microenvironment in metastasis: what is special about bone? 2008. Cancer Metastasis Reviews. 27:41-55.

Dhurjati, R., V. Krishnan, L.A. Shuman, A. M. Mastro, and E.A. Vogler. Metastatic Breast Cancer Cell Colonization Degrades Three-Dimensional Osteoblast Tissue *In Vivo.* Submitted to Clinical and Experimental Metastasis.

Shuman, L.A., V. Krishnan, R. Dhurjati, E.A. Vogler and A.M. Mastro. Metastatic Breast Cancer Cells Colonize and Penetrate Osteoblast Multilayers in a 3-D Culture System. Submitted to Cancer Research.

Abstracts/Presentations

Krishnan, V., Dhurjati R., Vogler E.A., and Mastro A.M. Osteoblast Maturity Modulates Metastatic Breast Cancer Colonization in a Novel Bioreactor. Skeletal Complications and Malignancy V. October 2007, Philadelphia, PA.

Krishnan, V., R. Dhurjati, L. A. Shuman, E. A. Vogler and A. M. Mastro. System in Crisis: In Vitro Model of Breast Cancer Colonization of Bone. *Bones and Teeth*, Gordon Research Conference. July 2007, University of New England, Biddeford, ME.

Krishnan,V., R.Dhurjati, L. A. Shuman, A. M. Mastro and E. A. Vogler. On the Permanent Life of Tissue Outside the Body. Annual Meeting of American Association for the Advancement of Science. February 2007, San Francisco, CA

Shuman, L.A. and A. M. Mastro. Mechanisms By Which Metastatic Breast Cancer Cells Inhibit Osteoblast Differentiation. Novartis xMAP® Technology Day. May 30, 2007, Boston, MA.

Shuman,L.A.and A.M.Mastro. TGF-B in Metastatic Breast Cancer Conditioned Medium Upregulates Egr and NFkB Transcription Factor Activities, Represses NFY1 Transcription Factor Activity, and Increases the Production of Inflammatory Cytokines in Osteoblasts. PAGET Foundation Symposium: Skeletal Complications of Malignancy V. October 25–27, 2007, Philadelphia, PA.

Shuman, L.A., V. Krishnan,R. Dhurjati, D.M., Sosnoski,E.A. Vogler, and A.M.Mastro, A physiologically relevant 3D *in vitro* tissue culture system for monitoring the interaction of metastatic breast cancer cells with osteoblasts. The American Association for Cancer Research Conference. April 12–16, 2008, San Diego, CA.

Dhurjati R., L.A. Shuman, V. Krishnan, A.M. Mastro, and E.A.Vogler. Metastatic Colonization of Bone Tissue by Breast Cancer *In Vitro.* 53rd Annual Conference of the American Society for Artificial Internal Organs. June 7-9, 2007, Chicago.

Dhurjati R., V. Krishnan, L.A. Shuman, A.M. Mastro, and E.A Vogler.. On the Permanent Life of Bone Tissue Outside the Organism. Gordon Research Conference on Bones and Teeth. July 15-20, 2007, Biddeford, ME.

Dhurjati R., V. Krishnan, L.A.Shuman, A.M. Mastro,. and E. A.Vogler. 3D Engineered Bone Tissue for the study of Osteogenesis and Breast Cancer Colonization of Bone. 54th Annual Meeting of the Orthopaedic Research Society. March 2-5, 2008, San Francisco, CA.

Thesis

Dr. Ravi Dhurjati received his Ph.D. in Materials Science and Engineering from The Pennsylvania State University in December of 2007. The title of his thesis was “On the Permanent Life of Tissue Outside of the Organism.”

CONCLUSIONS

The use of a specialized bioreactor has allowed us to grow osteoblasts for extended time, i.e. 10 months at least. Both primary osteoblasts and cell lines form a three dimensional mineralizing tissue. Challenge of the 3-D culture with breast cancer cells created a system that simulates metastatic breast cancer colonization of bone. Within hours the osteoblasts respond with an inflammatory stress response. They also show reduced expression of osteoblast differentiation genes. The cancer cells adhere to the osteoid- like tissue and penetrate the cell layer. The also cause loss of extracellular matrix. Both osteoblasts and cancer cells change to more spindle-shaped cells. The cancer cells line up in a pattern described as “Indian filing.”

REFERENCES

1. Bussard, KM. C.V. Gay, A.M. Mastro. The bone microenvironment in metastasis: what is special about bone? Cancer Metastasis Reviews. 2008; 27:41-55.

2. Dhurjati R, Liu X, Gay CV, Mastro AM, Vogler EA. Extended-Term Culture of Bone Cells in a Compartmentalized Bioreactor. Tissue Engineering 2006;12:3045-3054.

3. Kinder, M., E. Chislock, K.M. Bussard, L. Shuman, and Andrea M. Mastro. Metastatic breast cancer induces an osteoblast inflammatory response. Exp, Cell Res. 2008; 314:173-189.

4. Liu, X., J.Y. Lim, H.J. Donahue, R. Dhurjati, A.M. Mastro, E.A. Vogler. Influence of substratum surface chemistry / energy and topography of the human fetal osteoblastic cell line. Biomaterials. hFOB1.19: phenotypic and genotypic responses observed in *in vitro*. 2007;28:4535-4550.

5. Mercer R, Miyasaka C, Mastro A. Metastatic breast cancer cells suppress osteoblast adhesion and differentiation. Clin Exp Metastasis 2004;21:427-35.

6. Mercer R, and Mastro AM. Cytlines secreted by bone-metastatic breast cancer cells alger the expression pattern of f-actin and reduce focal adhesion plaques in osteoblasts through PI3K. Exp. Cell Res. 2005; 310: 270-281.

APPENDIX

Dhurjati, R., V. Krishnan, L.A. Shuman, Andrea M. Mastro, and E.A. Vogler. Metastatic Breast Cancer Cell Colonization Degrades Three-Dimensional Osteoblast Tissue *In Vivo.* Submitted to Clinical and Experimental Metastasis.

Shuman, L.A., V. Krishnan, R. Dhurjati, E.A. Vogler and A.M. Mastro. Metastatic Breast Cancer Cells Colonize and Penetrate Osteoblast Multilayers in a 3-D Culture System. Submitted to Cancer Research.

APPENDICES

Manuscript # 1

(DRAFT)

Metastatic Breast Cancer Cell Colonization Degrades Three-Dimensional Osteoblastic Tissue *In Vitro*

A Contribution from the Osteobiology Research Group
The Pennsylvania State University

Ravi Dhurjati[†a], Venkatesh Krishnan[Φa], Laurie A. Shuman[Φ], Andrea M. Mastro[Φ], and Erwin A. Vogler[†‡*]

Departments of Materials Science and Engineering[†], Bioengineering[*] and Biochemistry and Molecular Biology[Φ]

Materials Research Institute and the Huck Institutes of Life Sciences[‡], Pennsylvania State University, University Park, PA 16802.

[*] **Author to whom correspondence should be addressed:** EAV3@PSU.EDU

[a] Authors contributed equally

Keywords: bone metastases, breast cancer, colonization, inflammation, invasion, osteoblast, three-dimensional cell culture model

Abstract

Metastatic breast cancer cells (BCs) colonize a mineralized three-dimensional (3D) osteoblastic tissue (OT) grown from isolated pre-osteoblasts for up to 5 months in a specialized bioreactor. Sequential stages of BC interaction with OT include BC adhesion, penetration, colony formation, and OT reorganization into “files” paralleling BC colonies, heretofore, observed only in authentic pathological breast tissue. BCs permeabilize OT by degrading the extra-cellular collagenous matrix (ECM) in which the osteoblasts are embedded. OT maturity (characterized by culture age and cell phenotype) profoundly affects the patterns of BC colonization. BCs rapidly form colonies on immature OT (higher cell/ECM ratio, osteoblastic phenotype) but fail to completely penetrate OT. By contrast, BCs efficiently penetrate mature OT (lower cell/ECM ratio, osteocytic phenotype) and marshal OB into files. BC colonization provokes a strong osteoblast inflammatory response marked by increased expression of the pro-inflammatory cytokine IL-6. Furthermore, BCs inhibit osteoblastic bone formation by down-regulating synthesis of collagen and osteocalcin. Results strongly suggest that breast cancer disrupts the process of osteoblastic bone formation, in addition to upregulating osteoclastic bone resorption as reported. These observations may help explain why administration of bisphosphonates to humans with osteolytic metastases slows lesion progression by inhibiting osteoclasts but does not bring about osteoblast-mediated healing.

Introduction

Skeleton is a favored site for the metastatic spread of breast, prostrate, lung, and multiple myeloma cancers [1]. Metastatic cancer in bone is particularly pernicious because, once bone colonization occurs, the cure rate is almost zero [1-3]. Cancers in bone progress with significant morbidity related to bone loss (lytic cancer) or gain (blastic cancer), hypercalcemia, pathological fractures, and spinal compression [3]. Specific aspects of cancer-cell growth in bone such as dormancy [4, 5] contribute to a protracted disease progression with intervals of remission that can sometimes last up to decades [6]. Metastatic colonization of bone is the culmination of a sequence of steps beginning with migration of cancer cells to bone, survival and adaptation to the bone environment, proliferation to form micrometastases, and finally development of vascularized tumors [7]. Successful progression through these different stages requires reciprocal interactions between cancer cells and the bone microenvironment [8]. Of the cancer cells that reach bone, only a small percentage of cells develop into clinically detectable tumors; the remaining either die, persist as solitary dormant cells, or develop into pre-angiogenic micrometastases that fail to develop into overt tumors [7, 9].

The specific cellular and molecular mechanisms responsible for the variable fate of cancer cells in bone are incompletely understood [7]. Investigations of metastasis suppressor genes [10] and cell trafficking studies using intravital videomicroscopy [11, 12] have revealed that early stage, pre-angiogenic interactions between the cancer cells and the bone environment are crucial regulators of cancer-cell growth and disease progression. Evidence from these two independent lines of investigation suggest that early stages of metastatic colonization constitute a rate-limiting step in disease progression that can be an effective target for therapeutic intervention [13]. Consequently, a full appreciation of the mechanistic basis of metastatic

colonization can greatly enhance discovery of drugs aimed at the arrest of cancer-cell growth that will limit disease progression to a minimal residual, asymptomatic stage [14].

One difficulty encountered in drug development is that early-stage detection of cancer-cell colonization is difficult, both in the clinic and laboratory, because of the refractory nature of whole bone and lack of relevant *in vitro* models, respectively. Excised tissue [15] faithfully captures end stages of cancer in bone associated with fully-developed tumors, but the critical initial stages of disease remain largely inaccessible in this surrogate. Effective *in vitro* bone models must strike a balance between experimental efficiency and retention of biological complexity. In particular, the model must recapitulate the *in vivo* bone microenvironment to the greatest extent possible. Three-dimensional (3D) tissue models have become a focus of recent investigation for this reason [16]. Herein, we report use of a multiple-cell layer (3D) mineralizing osteoblastic tissue (OT) grown from isolated osteoblasts in a specialized bioreactor as an effective surrogate for studies of cancer colonization of bone. By challenging OT with metastatic breast cancer cells (BCs) known to invade the skeleton, important hallmarks of the metastatic process including cancer cell/tissue adhesion, tissue penetration, and ultimate degradation of the osteoblast-derived extracellular matrix were directly observed *in vitro*.

Materials and Methods

Bioreactor Design and Implementation: Bioreactors based on the principle of simultaneous-growth-and-dialysis [17, 18] were implemented using a two-compartment bioreactor design described previously [19, 20]. One of the compartments was a cell-growth chamber (5 mL total volume) that was separated from a 30 mL medium-reservoir compartment by a dialysis membrane (6-8KD cutoff). Cells were inoculated into the growth chamber in complete medium including serum. The reservoir was filled with basal medium consisting of nutrients such as glucose and amino acids but no proteins. The entire vessel was ventilated through transparent, gas-permeable but liquid-impermeable films that offered optimum cell adhesion and delivered requisite oxygen tension to the cells. The bioreactor was specifically designed to enable non-invasive, live-cell analysis with an inverted (phase-contrast, fluorescence, or confocal) microscope. Completely assembled units used in this work had a cell-growth space of 25 cm^2 total area emulating a standard T25 flask. Bioreactors were sterilized by gamma radiation at the Breazeale Nuclear Reactor on the campus of The Pennsylvania State University.

During culture, cells were bathed in pH-equilibrated and oxygenated medium that continuously dialyzed from the medium reservoir. At the same time, metabolic waste products such as lactic acid dialyzed out of the growth compartment, maintaining low pericellular concentrations. The medium reservoir was designed to be periodically replenished to provide additional nutrients and remove accumulated waste products without disturbing the cell growth chamber. Serum constituents or macromolecules synthesized by cells with molecular weights in excess of the dialysis membrane cutoff (8-10 kDa) were retained and concentrated within the growth compartment. This simple-to-use bioreactor design was integrated into conventional tissue culture protocols. The system conferred an extraordinarily stable pericellular environment that improved cell recovery from “culture shock” [21], and resulted in development of osteoblastic tissue with a normal phenotype over extended, uninterrupted culture intervals tested for as long

as 10 months with no sign of necrosis [19, 20]. Tissue with up to 5 month maturity was utilized in this work.

Cells and Cell Culture: Murine calvarial pre-osteoblasts (MC3T3-E1) were a gift from Dr. Norman Karin at the Pacific Northwest National Laboratories (ATCC CRL-2593 presumptive equivalent). MC3T3-E1 were inoculated into the growth chamber of the bioreactors at a sub-confluent density (10^4 cells/cm^2) and cultured in alpha minimum-essential medium (α-MEM) (Mediatech, Herdon, VA) supplemented with 10% neonatal FBS (Cansera, Roxdale, Ontario) and 100 U/ml penicillin and 100 µg/ml streptomycin (Sigma Aldrich, St. Louis, MO). The medium reservoir of the bioreactor was filled with α-MEM supplemented with 100 U/ml penicillin and 100 µg/ml streptomycin but no serum. Once the cells reached confluence, usually 4-5 days, the medium in the growth chamber was replaced with differentiation medium containing the additional ingredients of 50 µg/mL ascorbic acid and 10 mM β-glycerophosphate (Sigma Aldrich, St. Louis, MO). This change to differentiation medium was the only time during the course of the experiment that medium in the cell chamber was replaced. Subsequent medium changes involved only the basal medium within the medium reservoir that was refreshed every 30 days. Bioreactors were maintained in a water-jacketed 5% CO_2 incubator (Model 3110, Thermo Fisher Scientific, Waltham, MA) held at 37 ^oC. In this way, MC3T3-E1 cultures have been maintained continuously in the bioreactor without sub-culture for extended intervals up to 10 months, generating a multiple-cell layer tissue with controllable age (maturity), herein referred to as osteoblastic tissue (OT).

Human metastatic breast cancer cells (MDA-MB-231, ATCC-HTB 26 presumptive equivalent) genetically engineered to produce green fluorescent protein (GFP), were a gift from Dr. Danny Welch, University of Alabama at Birmingham, and herein referred to as BCs. Derived from a pleural effusion [22], MDA-MB-231^{GFP} cells are known to invade the murine skeleton [23]. MDA-

MB-231^{GFP} cells were cultured in standard tissue culture dishes in Dulbecco's Modified Eagle's Medium (DMEM) (Mediatech, Herdon, VA) containing 5% fetal bovine serum and 100U/ml penicillin and 100µg/ml streptomycin for 3-4 days before co-culture with bioreactor-derived OT.

Reverse Transcription Polymerase Chain Reaction: MC3T3-E1 cells were cultured in the bioreactor for various intervals (7, 22, 30, 60 days). At the desired OT maturity, cells were harvested from the bioreactor and RNA isolated (RNeasy, Qiagen, Valencia, CA). RNA purity was determined by the A260/ A280 ratio; all samples had a ratio >1.8. CDNA was generated from 1 µg RNA using RETROscript kit (Ambion, Austin, TX). PCR was carried out on a thermocycler [DetaCycler 1™ System (Ericomp San Diego, CA)]. The sequences of the PCR primer pairs used for amplification are listed in Table 1. PCR reactions were run on a 2% agarose gel, stained with ethidium bromide and imaged under UV illumination. Ethidium bromide stained bands were quantitated using Imagequant software (Molecular Dynamics, Sunnyvale, CA) and normalized to β-actin.

Bioreactor Co-Cultures: BCs were inoculated into bioreactor cell-growth chambers containing OT at maturities between 15 and 145 days of culture at and an estimated 1:10, 1:100, or 1:1000 breast cancer-to-osteoblast cell ratio; corresponding to 10^5, 10^4 , or 10^3 BCs/bioreactor, respectively. BC challenged bioreactors were monitored microscopically for 7 days. On day 7, bioreactors were dismantled and substratum film with adherent tissue was carefully cut into pieces for various assays, avoiding loss of OT that was conspicuously degraded by BC challenge. Medium from the cell growth space of the bioreactor was collected and used for various analyses. Tissue was fixed in 2.5% glutaraldehyde (in cacodylate buffer) and stained for actin filaments with Alexa Fluor 568 phalloidin stain (Invitrogen, Carlsbad, CA). Osteoblasts were optionally stained with Cell Tracker Orange™ (Invitrogen, Carlsbad, CA) for live *in situ* confocal imaging to monitor cell growth dynamics, prior to staining with actin stain.

Conditioned Media Experiments: BCs were grown to 90% confluency in standard tissue culture plates and growth medium was removed. Adherent BCs were rinsed with PBS and the original growth medium replaced with fresh α-MEM (20 ml in a T-150 flask, ~1.3 x 10^5 cells/cm^2). Cultures were incubated for an additional 24 hours, the medium collected and centrifuged (300x g for 10 minutes) to remove cellular debris resulting in "BC-conditioned medium". At desired OT maturity, medium in the growth chamber of the bioreactor was completely replaced with breast-cancer conditioned medium. Osteoblast tissue in the bioreactor was exposed to BC-conditioned medium for 2 weeks.

Confocal Microscopy: *In situ* laser-scanning confocal microscopy of co-cultures in the bioreactor was performed using Olympus FV-300 laser scanning microscope (Olympus America Inc., Center Valley, PA). Sections were observed with a 40X Olympus UPlanF1 objective with an 0.85 numerical aperture. Cell Tracker Orange ™ was excited using a 543 nm line from a helium-neon laser and collected through a 565 nm long-pass filter. GFP was excited using a 488 nm argon laser and collected through 510 nm long-pass and 530nm short-pass filters. A 570nm dichroic long-pass filter was used to split the emission. Serial optical sections were taken at 1µm intervals throughout the tissue. Confocal images were processed using image processing software (Fluoview 300, Version 4.3b, Olympus, Center Valley, PA). 3D optical reconstructions of 2-D serial sections were obtained using AutoQuant, AutoDeblur and AutoVisualize software (Version 9.3, Media Cybernetics, Bethesda, MD). Number of cell layers

Dhurjati *et al* *Cancer Colonization of Osteoblastic Tissue* page 8

within the tissue was determined visually by counting and by following the sub-volumes of cells in the 3D-reconstructed Z-stack images.

Biochemical Assays: Soluble collagen (indicative of collagen synthesis) was quantified using Sircol Assay (Biocolor, Carrickfergus, UK). Prior to running the assay following manufacturer's

protocol, the collagen was extracted/ precipitated from cell culture supernatants by addition of 4M NaCl. Supernatants were centrifuged and the resulting collagen pellet was re-suspended in 0.5 M acetic acid. Levels of osteocalcin and IL-6 secreted into the medium were quantified using multiplex ELISA kit (LINCOplex™ Mouse Bone Panel 2B, Millipore, Billerica, MA).

Results

Osteoblast Tissue Model: Murine MC3T3E-1 pre-osteoblasts maintained in the bioreactor developed into a 3D osteoblast tissue (OT, Panel A of Figure 1) comprised of 6-8 layers of differentiated cells (Panels B, top layer; Panel C, bottom layer) that stained positive for alkaline phosphatase activity and for mineralization by von Kossa (not shown). Continuous culture in the bioreactor resulted in transformation of spindle shaped pre-osteoblasts (Figure 2, Panel A) to cuboidal osteoblasts (Panel B) that secreted and mineralized an extensive, collagenous extracellular matrix (Panel C) that completely enveloped cells (Panel D). Examination of numerous histological and ultra-structural (not shown), and confocal sections of tissue from bioreactor cultures at different times revealed reproducible and continuous transformation of tissue in which cells were initially closely packed (high cell/ECM ratio; Figure 2 Panel A) to a more mature phenotype characterized by lower-cell density (low cell/ECM ratio; Figure 2 Panels C,D) with intercellular contacts maintained by a network of cellular processes [20]. Growth and maturation of OT in the bioreactor thus recapitulated the normal sequence of bone development characterized by stages of proliferation, matrix maturation, and mineralization. This phenotypic progression was also reflected in the characteristic expression of genes such as Type I collagen, osteonectin, osteocalcin and osteopontin (Figure 2, Panel E) [24]. Up-regulation of matrix-metallo protease (MMP)-13 (indicative of extracellular matrix remodeling) and the protein E11 (indicative of osteocytic transformation) occurred in mature cultures (Figure 2, Panel E).

Breast Cancer Cell Challenge to Osteoblast Tissue: Interaction of cancer cells with OT were followed by fluorescence microscopy after injecting MDA-MB-231 GFP human breast cancer cells directly onto 5-month OT stained with Cell Tracker Orange™ to clearly differentiate osteoblasts from cancer cells. BCs adhered to OT (Figure 3 Panel A) and penetrated tissue (Panel B) within the first 24 hours, apparently through the agency of cellular processes extended by BCs. Within 2 days of co-culture, BCs proliferated and organized into files (Panels C). Close inspection of 2D optical sections (Figure 4, Panel A, Day 3) and 3D reconstructions (Figure 4, Panel D) revealed concomitant re-organization of OT. Before cancer-cell challenge, osteoblasts exhibited a cuboidal morphology. Over 3 days of BC co-culture, osteoblasts took on a definitively elongated appearance and aligned with cancer cells which also became spindle shaped (filing). In particular, osteoblasts paralleled the BC cells, as though marshaled into an order that seemed to permeabilize OT structure. The BC alignment in the bioreactor was reminiscent of the classical “Indian filing” pattern that is one of the defining characteristics of breast cancer invasion [25-27].

Breast Cancer Cell Conditioned Medium Effects on Osteoblast Tissue: Prior work determined that exposure of MC3T3-E1 cells to conditioned medium (CM) from MDA-MB-231 cells caused a change in osteoblast morphology and adherence to the substrate under standard tissue culture conditions [28]. In order to determine if this effect occurred with 3D OT, 16 day OT in the bioreactor was maintained in CM for 2 weeks (see Methods and Materials). Exposure of OT to BC-conditioned medium induced significant cytoskeletal reorganization in response to factors secreted by BCs, as revealed by actin stress-fiber reorganization (Figure 3, compare contol Panel D to test Panel E). Control OT were characterized by smooth, long actin stress fibers (Panel D), whereas, F-actin stress fibers were clumped and punctate in OT exposed to conditioned medium (Panel E). These cytoskeletal changes correlated with the observation that OT from co-culture experiments was consistently more fragile than OT not exposed to cancer

cells. In fact, very careful processing was required to prevent wholesale cell sloughing during the wash steps involved in preparation of specimens for histology and electron microscopy. It was plainly evident from these latter observations that OT structure and adhesion to the bioreactor substratum film was significantly eroded by BC exposure. Details of BC interaction with OT were followed using the confocal microscopy study outlined in the legend to Figure 4 and as detailed in the Discussion Section.

Effect of Osteoblast Tissue Maturity on Breast Cancer Cell Interactions: The interaction of BC cells with OT depended on the stage of OT maturity,. As the OT matured, there was decrease in the number of cell layers with increasing culture time (Figure 5, left-hand axis of graphic portion) that translated into a linear-like decrease in cell-layer/tissue-thickness ratio (Figure 5, right-hand axis). Qualitative aspects of BC interactions were correlated with OT characteristics (Figure 5, table portion), suggesting that declining rates of BC colonization and increasing efficiency of tissue penetration, filing, and colony formation were related to OT maturity.

The effect of BCs on OT was further assessed by measuring the changes in levels of secreted factors representing primary osteoblast functions of extracellular matrix production (secreted collagen) and mineralization (osteocalcin). Introduction of breast cancer cells led to reduced production of new collagen (Figure 6, Panel A) and osteocalcin (Figure 6, Panel B) at all tested OT maturities. Furthermore, breast cancer cells stimulated increased production of IL-6, indicative of an inflammatory stress response (Figure 7) [29].

Discussion

Osteoblastic Tissue Model: A relatively simple bioreactor has been used to grow a three-dimensional (3D) osteoblastic tissue (OT) from isolated murine MC3T3E-1 pre-osteoblasts for culture periods up to 5 months. This extended culture interval allowed maturation of OT through successive stages of phenotypic development, up-to-and-including osteocyte-like cells. A morphologically-stratified tissue develops within the first month of culture (Figure 1; compare top layer Panel B to bottom layer Panel C). Over successive months of culture, cuboidal osteoblastic cells underwent continued morphological changes (Figure 2) accompanied by characteristic expression of genes such as Type I collagen, osteonectin, osteocalcin and osteopontin; as well as up-regulation of MMP-13 (suggestive of active matrix turnover) and protein E11 (indicative of osteocytic transformation). The number of cell layers comprising OT and tissue thickness decreased with culture time (Figure 5) in a manner consistent with the increased osteoblast apoptosis observed in the formation of natural bone [30]. These observations are collectively interpreted to mean that continuous culture of MC3T3-E1 cells in the bioreactor recapitulated growth and phenotypic development of native bone tissue *in vivo*, excluding osteoclast-mediated remodeling. Osteoclasts have been purposely excluded from the bioreactor-based model so that osteoblast biology could be clearly observed.

Breast Cancer Cell Challenge to Osteoblast Tissue: Confocal microscopy showed that MDA-MB-231 human breast cancer cells (BCs) adhered to and penetrated OT (Figures 3 and 4). BCs penetrated OT by extending long cellular protrusions that were enriched in filamentous actin and formed “Indian files” similar to that observed in infiltrating lobular or metaplastic breast carcinomas [25, 26]. Migration of cancer cells along tracks of remodeled ECM produced by preceding invading cell(s) results in characteristic filing patterns [27]. Invasion by files or chains of tumor cells linked together by cell-cell contacts is considered to be an effective penetration mechanism conferring high metastatic capacity and commensurately poor prognosis [25, 27].

Observation of BC invasion files in the OT model suggests a considerable degree of physiological relevance.

BC attachment and penetration varied significantly with OT maturity (Figure 5). BCs failed to penetrate immature OT (less than 30 days in culture); instead forming colonies substantially on, not in, OT. Significant penetration, remodeling, and characteristic cancer-cell filing patterns were observed only in relatively mature OT. We speculate that BC penetration is inhibited by close contacts among osteoblasts comprising immature OT and becomes more efficient as the cell/ECM ratio decreases, creating a more permeable tissue. The first penetrating BC remodels the extracellular matrix in a way that creates a path for other BCs [31], leading to the files of cells as discussed above. This progressive process marshals OT into a pattern that paralleled BC files.

Unlike conventional cell culture wherein continuous or scheduled medium exchanges lead to loss of cell secreted growth factors and cytokines, the compartmentalized bioreactor retains all factors secreted into the cell-growth compartment that have molecular weight greater than 6-8KD dialysis-membrane cutoff (see Methods and Materials). We believe this attribute is critical to simulating the bone microenvironment because osteoblasts are known to secrete a number of growth factors and cytokines in a spatially and temporally ordered sequence that is closely aligned with the specific stages in osteoblast development [24]. Likewise, BC co-culture introduces growth factors and cytokines that would presumably concentrate in the microenvironment in physiological conditions. For these reasons, we maintain that the OT model is a relevant model for cancer colonization of bone.

Osteoblast Inflammatory Response: Inflammation is linked closely with the progression of many cancers [32]. Osteoblasts are able to mount an inflammatory response independent of

immune cells [33]. Inflammation appears to play a critical role in bone loss in osteomyelitis due to bacterial infection in the bone [33] and in debris-mediated bone loss associated with titanium implants [34]. Previous studies in conventional culture have shown that exposure to BC-conditioned medium produced a profound osteoblastic inflammatory stress response that included increased expression of the inflammatory cytokines, IL-6, IL-8 and MCP-1 [35]. These cytokines are known to attract and activate osteoclasts, and are likely to contribute to the tumor-host microenvironment *in vivo*. In particular, IL-6 a pleiotropic cytokine [36], has been implicated in pathogenesis of osteolysis associated with Paget's disease [37], Gorham-Stout syndrome [38], and multiple myeloma [39]. IL-6 levels in breast cancer patients have been found to correlate to the clinical stage of the disease [40, 41] as well to the rate of recurrence [42]. High IL-6 serum levels in breast cancer patients were found to be an unfavorable prognosis indicator [43-45]. We thus interpret pronounced IL-6 production by OT in co-culture experiments (Figure 7) as a strong osteoblast inflammatory provoked by the presence of BCs. The concomitant decrease in collagen and osteocalcin secreted by OT co-cultured with BCs confirms that BC suppress osteoblast function in a manner consistent with inflammation-induced bone loss observed in bone pathologies.

Breast-Cancer Induced Bone Loss: Cancer-related bone loss appears to occur through multiple pathways. Evidence for osteoclast-mediated resorption is indeed very strong [46]. In addition, destruction of devitalized bone directly by cancer cells has also been reported [47], especially late in metastasis when bone-degradation rate is highest and osteoclast cell numbers are in decline [48]. These lines of evidence support the idea that osteoclasts are not solely responsible for excessive bone degradation and that cancer cells may directly contribute to bone loss. Degradation of the osteoblast tissue by co-culture with breast cancer cells observed in the bioreactor model (that purposely excludes osteoclasts) strongly suggests that yet another mechanism of bone loss is related to disruption of the bone-accretion process by destruction of

osteoblastic tissue. There is clinical and experimental literature to support this concept. For example, quantitative histomorphometric analyses of bone biopsies from patients with hypercalcemia due to bone metastasis indicated a dramatic decrease in osteoblast activity [49]. Histomorphometric analysis of rodents inoculated with lytic human breast cancer cells (MDA-MB-231) indicated that, even though administration of risedronate (a bisphosphonate) reduced the number of osteoclasts, slowed bone lysis, and significantly reduced tumor burden, there was no evidence of new bone deposition or repair [50]. Similarly, administration of bisphosphonates to humans with osteolytic metastasis slowed lesion progression but did not bring about healing [51]. Our previous work *in vivo* and *in vitro* also indicate that metastatic breast cancer cells suppress osteoblast adhesion and differentiation and increase osteoblast apoptosis [28, 48, 52]. All taken together, these observations strongly suggest that normal osteoblast function (i.e. deposition and mineralization of matrix) is not only impaired in the presence of breast cancer cells but, in fact, osteoblastic tissue is degraded by breast cancer invasion, possibly by enlisting a cooperative inflammatory response by osteoblasts themselves. Further understanding of the cellular and molecular basis for breast cancer colonization of bone and discovery of therapeutic interventions will be greatly expedited by the use of three-dimensional tissue models such as the one demonstrated in this study.

Acknowledgments: This work was supported by U.S. Army Medical Research and Material Command Breast Cancer Research Program WX81XWH-06-1-0432, and the Susan G. Komen Breast Cancer Foundation BCTR 0601044, National Foundation for Cancer Research, Center for Metastasis Research, The University of Alabama-Birmingham. Authors appreciate the expert technical assistance of Ms. Donna Sosnoki and the assistance of the Cytometry Facility and the Electron Microscopy Facility at the Huck Institutes of Life Sciences, Penn State University.

List of Figure Legends:

Figure 1: Phalloidin-stained MC3T3-E1 osteoblast-derived tissue (OT) after 22 days of continuous culture in the bioreactor. MC3T3-E1 pre-osteoblasts grow into a 3D osteoblastic tissue comprised of 6-8 cell layers enmeshed in a collagenous matrix (see also Figures 2,5). Panel A is a 3D reconstruction of serial confocal optical sections (magnification = 40X, scale bar = 100 µm). A morphological gradient in the tissue was evident wherein top layer of cells (Panel B) were conspicuously more cuboidal than bottom layer of cells (Panel C) which exhibited filamentous inter-cell connections reminiscent of osteocyte morphology.

Figure 2: Maturation of MC3T3-E1 derived OT within the bioreactor (see also Figures 1,5). Panels (A-D) are confocal images of actin-stained cells over several months of continuous culture (scale bar = 50 µm, annotations give culture age). Spindle-shaped pre-osteoblasts (Panel A) progressively transformed into cuboidal osteoblasts (Panel B) that became enmeshed in a collagenous matrix (Panel C appearing black) that eventually buried cells exhibiting an osteocytic-like morphology (Panel D). Expression of various osteoblast differentiation markers was determined by RT-PCR as a function of culture interval (Panel E, insets show ethidium-bromide stained bands for markers listed in Panel E annotations). Changes in marker expression was consistent with progression of osteoblast phenotype through the stages of proliferation, matrix maturation and mineralization (indicated by vertical bars in Panel E).

Figure 3: MDA-MB-231^{GFP} breast cancer cell invasion of MC3T3-E1 derived OT grown for 5 months within the bioreactor. OT (stained with Cell Tracker Orange^{TM}) was co-cultured with MDA-MB-231 breast cancer cells (BCs) genetically engineered to produce GFP. Confocal images (scale bar =50µm, magnification=40X) were collected over 3 days (Panels A-C). These

representative images are interpreted as stages of BC adhesion (Panel A), penetration (Panel B), and replication/organization into characteristic filing patterns (Panel C), respectively (see also Figure 4). Panels D, E compare phalloidin-stained OT grown for 16 days in the bioreactor to similar tissue exposed to MDA-MB-231 conditioned medium for 2 weeks (scale bar =50µm, magnification=40X). Note that exposure to conditioned media disrupted actin fiber organization in OT. Draq5 (Biostatus, Shepshed, UK) stained nuclei (blue) reveal concomitant nuclear shrinkage.

Figure 4: MDA-MB-231 breast cancer cell (BC) invasion of MC3T3-E1 derived osteoblastic tissue (OT) grown for 5 months within the bioreactor (see also Figures 1, 3). BCs were added to a 5 month OT culture as described as in the legend to Figure 3. Optical sections (40X, scale bar = 50µm) at various depths within OT at successive days in culture were collected by laser scanning confocal microscopy. It is evident that BCs fully penetrated OT only in a few locations within day 1 of co-culture. Penetration increased over days 2 and 3. Linear-like organization of breast cancer cells and osteoblasts was evident within the tissue beginning at day 2 but apparent at day 3. Optical reconstructions of serial sections over 3 days (Panels B-D respectively, 40X) revealed significant re-organization and permeablization of OT.

Figure 5: Qualitative aspects of MDA-MB-231 metastatic breast cancer cell (BC) interaction correlate with MC3T3-E1 derived OT maturity. An exponential-like decrease in the number of cell layers with time (left-hand axis, graph) translated into a linear-like decrease in cell-layer/tissue-thickness ratio (right-hand axis, graph). This observation was consistent with the process of bone-tissue maturation that resulted in transformation of proliferating pre-osteoblasts into non-dividing osteoblasts that become engulfed in mineralized matrix that mature into osteocytes through a process of phenotypic transformation marked by increased osteoblast apoptosis [30]. The data presented in the table suggested that declining rates of BC

colonization and increasing efficiency of tissue penetration, filing, and colony formation were related to OT maturity.

Figure 6: MDA-MB-231 metastatic breast cancer cells (BC) reduce production of osteoblast maturation markers by MC3T3-E1 derived osteoblast tissue (OT) grown in the bioreactor for 0.7, 1.2 and 2.2 months. Breast cancer cells (BC) were injected onto OT at a 1:10 BC-to-osteoblast cell ratio and co-cultured for 7 days. OT with no added BC served as controls. Levels of soluble collagen secreted by osteoblasts into the medium in the presence and absence of breast cancer cells were quantified using Sircol™ Assay (Biocolor) ($n \geq 2$). Levels of osteocalcin secreted into the medium in the presence and absence of breast cancer cells were quantified using multiplex ELISA assay (LINCOplex™ Mouse Bone Panel 2B, Millipore). Shown are averages of duplicate sample determination.

Figure 7: MDA-MB-231 metastatic breast cancer cells induce inflammatory response in osteoblast tissue in the bioreactor. MC3T3-E1 derived osteoblast tissue (OT) was grown in the bioreactor to desired maturity (0.7, 1.2 and 2.2 months). Breast cancer cells (BC) were then injected onto OT at 1:10 BC-to-osteoblast cell ratio and co-cultured for 7 days. OT with no added BC served as controls. Levels of the pro-inflammatory cytokine, IL-6 secreted by osteoblasts into the medium in the presence and absence of breast cancer cells were quantified using multiplex ELISA assay (LINCOplex™ Mouse Bone Panel 2B, Millipore). Shown are averages of duplicate sample determination.

Citations

1. Rubens RD, Mundy GR (2000) Cancer and the skeleton. London: Martin Dunitz
2. Rubens RD (1998) Bone metastases-the clinical problem. European Journal of Cancer; 34: 210-213
3. Nielsen OS, Munro AJ, Tannock IF (1991) Bone metastases: Pathophysiology and management policy. J Clin Oncol; 9 (3): 509-524
4. Aguirre-Ghiso JA (2007) Models, mechanisms and clinical evidence for cancer dormancy. Nat Rev Cancer; 7 (11): 834-846
5. Demicheli R (2001) Tumour dormancy: Findings and hypotheses from clinical research on breast cancer. Semin Cancer Biol; 11: 297-306
6. Kvalheim G, Naume B, Nesland JM (1999) Minimal residual disease in breast cancer. Cancer Metastasis Rev; 18: 101-108
7. Chambers AF, Groom AC, MacDonald IC (2002) Dissemination and growth of cancer cells in metastatic sites. Nature reviews Cancer; 2 (8): 563-572
8. Mundy GR (2002) Metastasis to bone: Causes, consequences and therapeutic opportunities. Nat Rev Cancer; 2: 584-593
9. Holmgren L, O'Reilly MS, Folkman J (1995) Dormancy of micrometastases: Balanced proliferation and apoptosis in the presence of angiogenesis suppression. Nature Med; 1: 149-153
10. Welch DR, Steeg PS, Rinker-Schaeffer CW (2000) Molecular biology of breast cancer metastasis: Genetic regulation of human breast carcinoma metastasis.
11. Chambers AF, Naumov GN, Vantyghem SA, et al. (2000) Molecular biology of breast metastasis: Clinical implications of experimental studies on metastatic inefficiency. 400 - 407
12. Chambers AF, MacDonald IC, Schmidt EE, et al. (1995) Steps in tumor metastasis: New concepts from intravital videomicroscopy. 279 - 301
13. Steeg PS (2000) Molecular biology of breast metastasis: 'has it spread?' disarming one of the most terrifying questions. 396 - 399
14. Chambers AF, MacDonald IC, Schmidt EE, et al. (2000) Clinical targets for anti-metastasis therapy. 91 - 121
15. Welch DR (1997) Technical considerations for studying cancer metastasis in vivo. 272 - 301
16. Schmeichel KL, Bissell MJ (2003) Modeling tissue-specific signaling and organ function in three dimensions. 2377-2388
17. Rose GG (1966) Cytopathophysiology of tissue cultures growing under cellophane membranes. In Richter GW, Epstein MA (eds): Int rev exp pathology. New York: Academic Press; 111-178.
18. Rose GG, Pomerat CM, Shindler TO, et al. (1958) A cellophane-strip technique for culturing tissue in multipurpose culture chambers. J Cell Biol; 4 (6): 761-764
19. Vogler EA (1989) A compartmentalized device for the culture of animal cells. J Biomaterials, Artificial Cells, and Artificial Organs; 17: 597-610
20. Dhurjati R, Liu X, Gay CV, et al. (2006) Extended-term culture of bone cells in a compartmentalized bioreactor. Tissue Engineering; 12 (11): 3045-3054

Dhurjati *et al* *Cancer Colonization of Osteoblastic Tissue* page 20

21. Sorkin AM, Dee KC, Knothe Tate ML (2004) "Culture shock" From the bone cell's perspective: Emulating physiological conditions for mechanobiological investigations. Am J Physiol Cell Physiol; 287 (6): C1527-1536
22. Cailleau R, Olive M, Cruciger QV (1978) Long-term human breast carcinoma cell lines of metastatic origin: Preliminary characterization. In vitro; 14 (11): 911-915
23. Rusciano D, Burger M (2000) In vivo cancer metastasis assays. In Welch D (ed): Cancer metastasis: Experimental approaches: Elsevier; 207-242.
24. Lian JB, Stein GS (1992) Concepts of osteoblast growth and differentiation: Basis for modulation of bone cell development and tissue formation. Crit Rev Oral Biol Med; 3 (3): 269-305
25. Page DL, Anderson TJ, Sakamoto G (1987) Diagnostic histopathology of the breast. 219-222
26. Pitts WC (1991) Carcinomas with metaplasia and sarcomas of the breast. Am J Clin Pathol; 95: 623-632
27. Friedl P, Wolf K (2003) Tumour-cell invasion and migration: Diversity and escape mechanisms. Nat Rev Cancer; 3 (5): 362-374
28. Mercer R, Miyasaka C, Mastro AM (2004) Metastatic breast cancer cells suppress osteoblast adhesion and differentiation. Clin & Exp Metas; 21 (5): 427-435
29. Kinder M, Chislock E, Bussard KM, et al. (2008) Metastatic breast cancer induces an osteoblast inflammatory response. Exp Cell Res; 314 (1): 173-183
30. Franz-Odendaal TA, Hall BK, Witten PE (2006) Buried alive: How osteoblasts become osteocytes. Developmental Dynamics; 235 (1): 176-190
31. Stetler-Stevenson WG (1993) Tumor cell interactions with the extracellular matrix during invasion and metastasis. Annual review of cell biology; 9 (1): 541
32. Visser Kd, Coussens L (2006) The inflammatory tumor microenvironment and its impact on cancer development. Contrib Microbiol: 118-137
33. Marriott I (2004) Osteoblast responses to bacterial pathogens: A previously unappreciated role for bone-forming cells in host defense and disease progression. Immunologic Research; 30: 291-308
34. Fritz EA, Glant TT, Vermes C, et al. (2002) Titanium particles induce the immediate early stress responsive chemokines il-8 and mcp-1 in osteoblasts. J Orthop Res; 20: 490-498
35. Kinder M, Chislock E, Bussard KM, et al. (2008) Metastatic breast cancer induces an osteoblast inflammatory response. Experimental cell research; 314 (1): 173-183
36. Papanicolaou DA (1998) The pathophysiologic roles of interleukin-6 in human disease. Annals of internal medicine; 128 (2): 127
37. Roodman GD, Kurihara N, Ohsaki Y, et al. (1992) Interleukin 6. A potential autocrine/paracrine factor in paget's disease of bone. The Journal of clinical investigation; 89 (1): 46-52
38. Devlin RD, Bone HG, 3rd, Roodman GD (1996) Interleukin-6: A potential mediator of the massive osteolysis in patients with gorham-stout disease. The Journal of clinical endocrinology and metabolism; 81 (5): 1893-1897
39. Klein B, Zhang XG, Lu ZY, et al. (1995) Interleukin-6 in human multiple myeloma. Blood; 85 (4): 863-872

40. Kozlowski L, Zakrzewska I, Tokajuk P, et al. (2003) Concentration of interleukin-6 (il-6), interleukin-8 (il-8) and interleukin-10 (il-10) in blood serum of breast cancer patients. Roczniki Akademii Medycznej w Bialymstoku (1995); 48: 82-84
41. Benoy I, Salgado R, Colpaert C, et al. (2002) Serum interleukin 6, plasma vegf, serum vegf, and vegf platelet load in breast cancer patients. Clinical breast cancer; 2 (4): 311-315
42. Mettler L, Salmassi A, Heyer M, et al. (2004) Perioperative levels of interleukin-1beta and interleukin-6 in women with breast cancer. Clinical and experimental obstetrics & gynecology; 31 (1): 20-22
43. Salgado R, Junius S, I.Benoy, et al. (2003) Circulating interleukin-6 predicts survival in patients with metastatic breast cancer. 103 (5): 642-646
44. Zhang GJ, Adachi I (1999) Serum interleukin-6 levels correlate to tumor progression and prognosis in metastatic breast carcinoma. Anticancer research; 19 (2B): 1427-1432
45. Bozcuk H, Uslu G, Samur M, et al. Tumour necrosis factor-alpha, interleukin-6, and fasting serum insulin correlate with clinical outcome in metastatic breast cancer patients treated with chemotherapy. Cytokine; 27 (2-3): 58-65
46. Kozlow W, Guise TA (2005) Breast cancer metastasis to bone: Mechanisms of osteolysis and implications for therapy. J Mammary Gland Biol Neoplasia; 10 (2): 169-180
47. Sanchez-Sweatman OH, Lee J, Orr FW, et al. (1997) Direct osteolysis induced by metastatic murine melanoma cells: Role of matrix metalloproteinases. European journal of cancer; 33 (6): 918-925
48. Phadke PA, Mercer RR, Harms JF, et al. (2006) Kinetics of metastatic breast cancer cell trafficking in bone. Clinical cancer research; 12 (5): 1431-1440
49. Stewart AF, Vignery A, Silverglate A, et al. (1982) Quantitative bone histomorphology in humoral hypercalcemia of malignancy: Uncoupling of bone cell activity. J Clin Endocrinol Metab; 55: 219-227
50. Sasaki A, Boyce BF, Story B, et al. (1995) Bisphosphonate risedronate reduces metastatic human breast cancer burden in bone in nude mice. Cancer Res; 55 (16): 3551-3557
51. Lipton A (2000) Bisphosphonates and breast carcinoma: Present and future. Cancer; 88: 3033-3037
52. Mastro A, Gay C, Welch D, et al. (2004) Breast cancer cells induce osteoblast apoptosis: A possible contributor to bone degradation. J Cell Biochem; 91 (2): 265-276

Table 1: Primer sequences and experimental conditions for RT-PCR

Gene	Primers (F=Forward; R=Reverse)	Annealing Temperature (^{o}C)	Cycles	Amplicon Size (bp)
Osteocalcin	F: 5'- CAA GTC CCA CAC AGC AGC TT- 3'	55	23	370
	R: 5'- AAA GCC GAG CTG CCA GAG TT- 3'			
Osteonectin	F: 5'- CTG CCT GCC TGT GCC GAG AGT TCC-3'	55	17	653
	R: 5'- CCA GCC TCC AGG CGC TTC TCA TTC-3'			
Type I Collagen	F: 5'- TCT CCA CTC TTC TAG TTC CT- 3'	55	16	269
	R: 5'- TTG GGT CAT TTC CAC ATG- 3'			
MMP-13	F: 5'- GAT GAC CTG TCT GAG GAA G- 3'	58	21	357
	R: 5'- ATC AGA CCA GAC CTT GAA G- 3'			
β-Actin	F: 5'- CGT GGG CCG CCC TAG GCA- 3'	62	20	242
	R: 5'- TTG GCC TTA GGG TTC AGG- 3'			

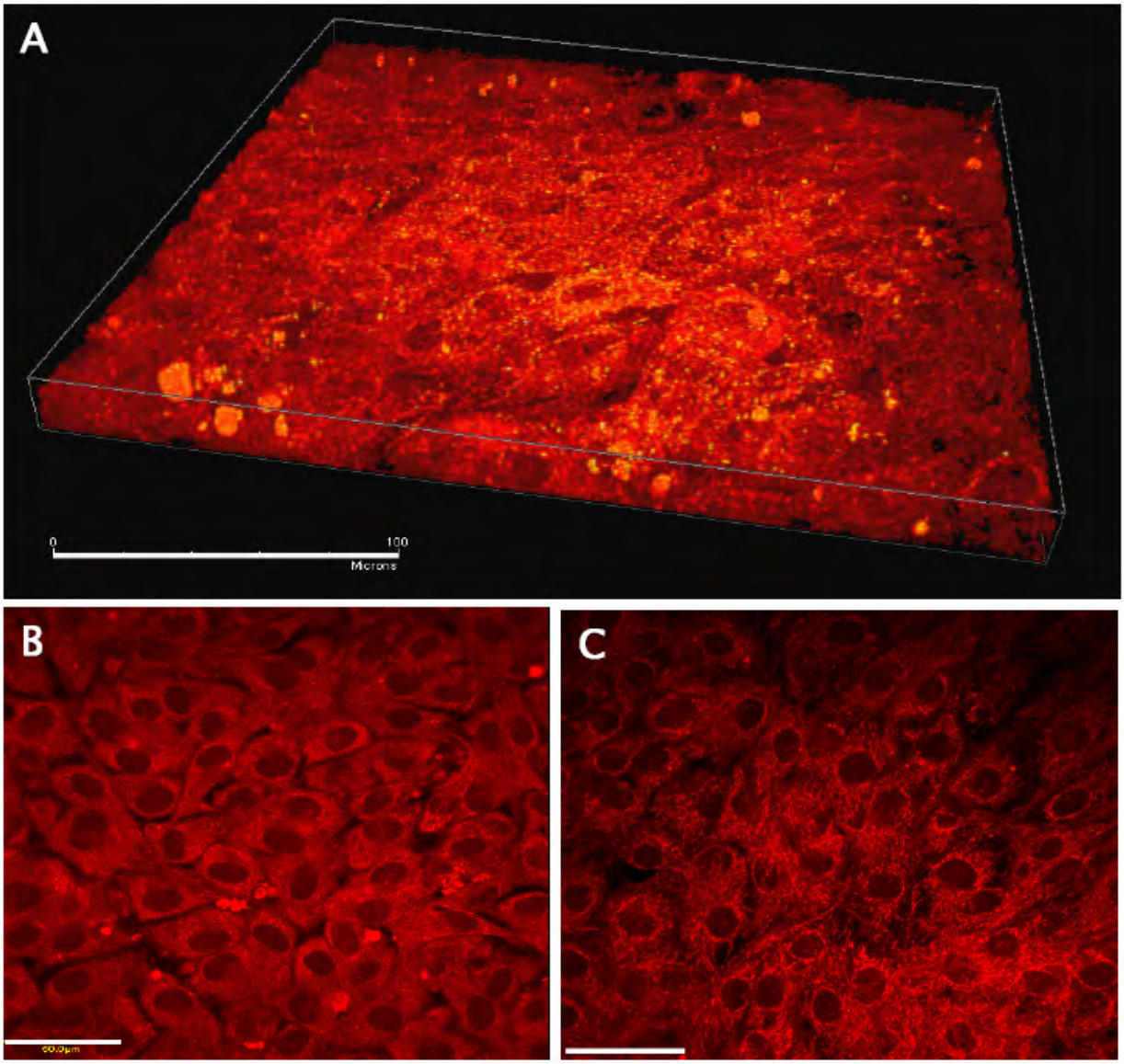
A
0
100
Microns
B
C

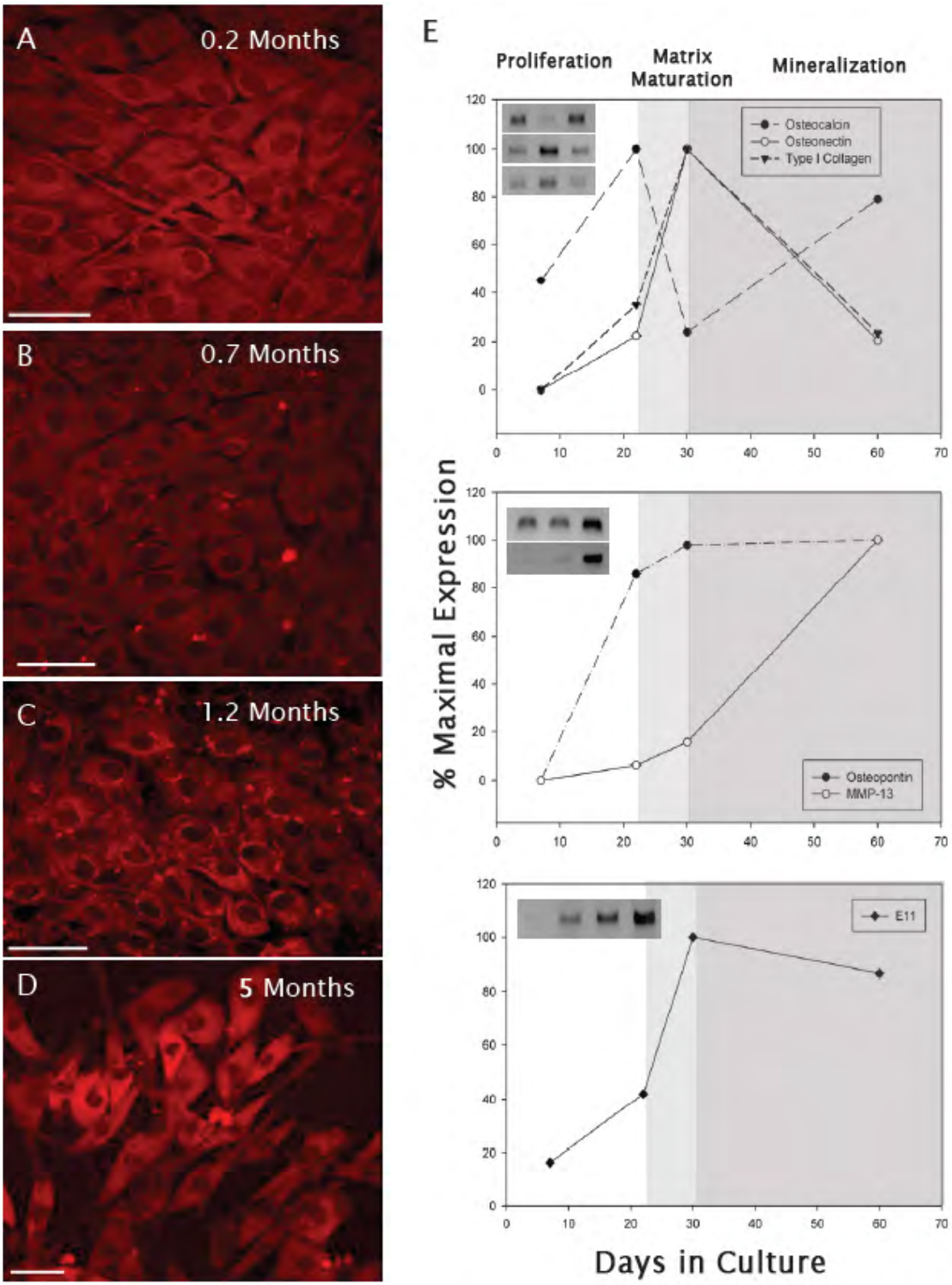
A
0.2 Months
B
0.7 Months
C
1.2 Months
D
5 Months
E
Proliferation
Matrix Maturation
Mineralization
Osteocalcin
Osteonectin
Type I Collagen
Osteopontin
MMP-13
E11
% Maximal Expression
Days in Culture

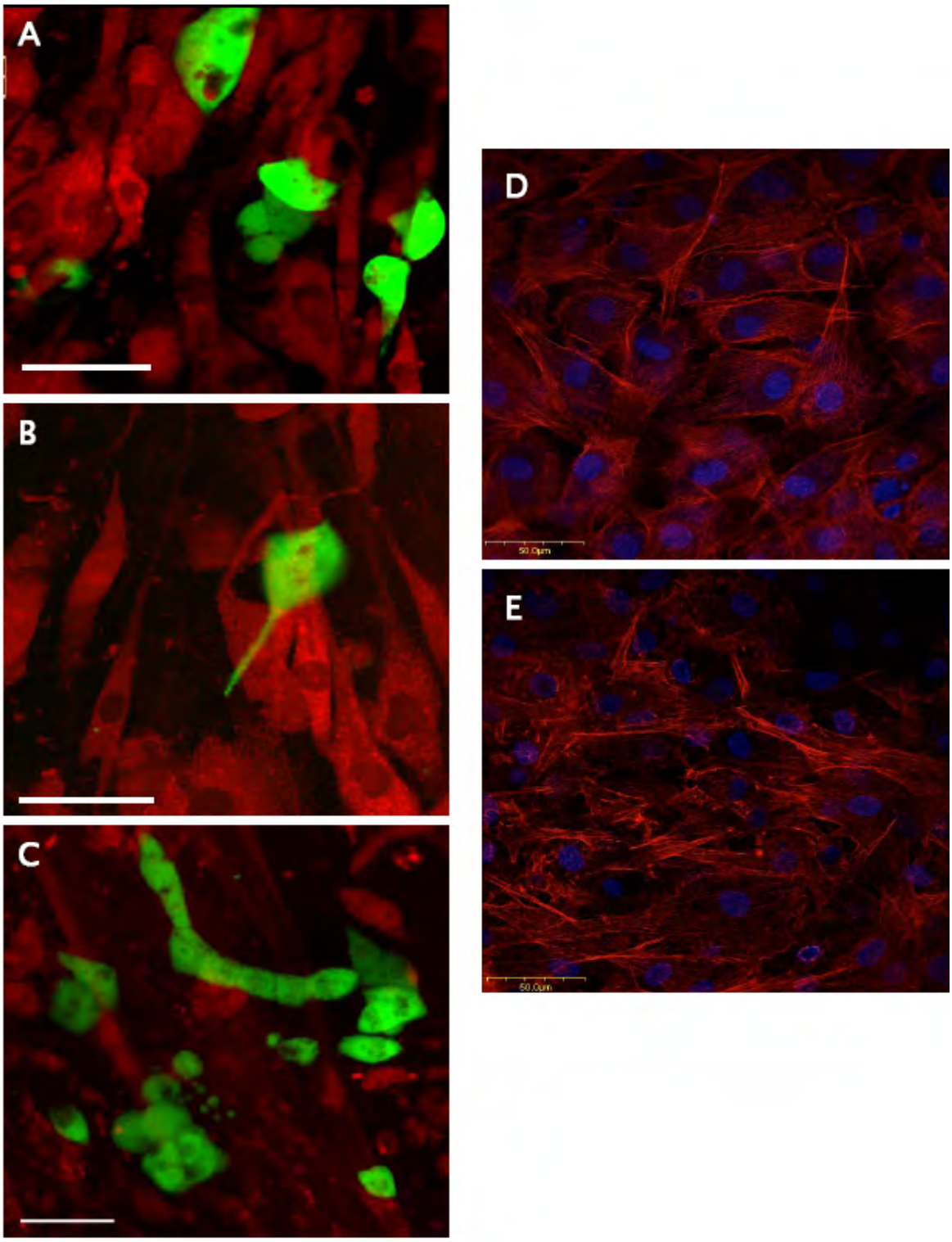
A
B
C
D
E

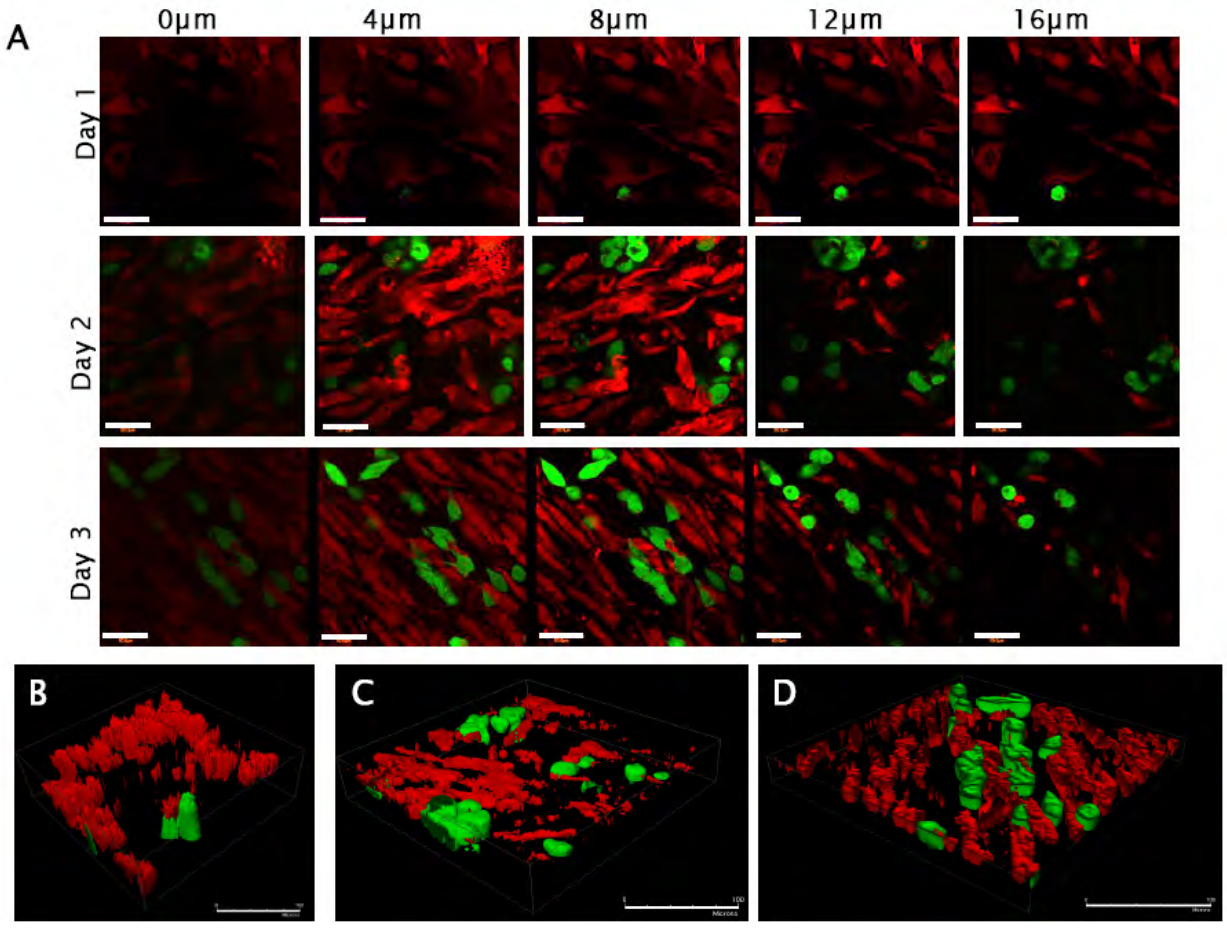
A
0µm
4µm
8µm
12µm
16µm
Day 1
Day 2
Day 3
B
C
D

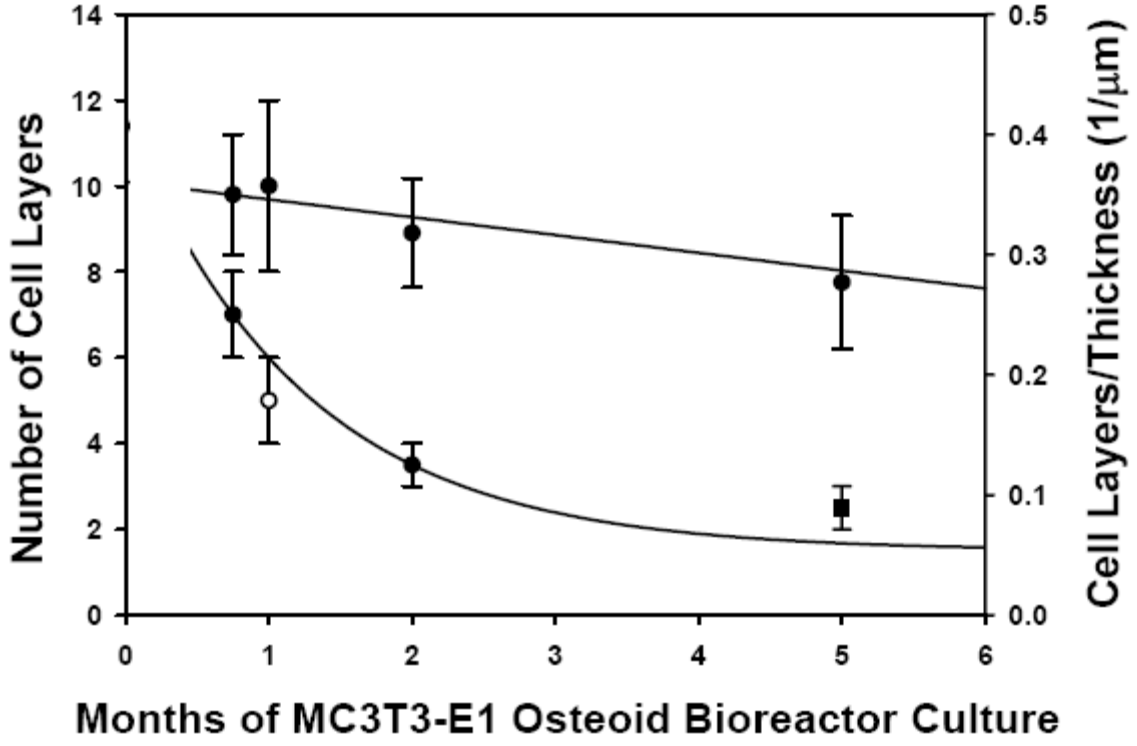

Experimental Parameter @ BC:OB=1:10	Months of Bioreactor Culture			
	0.75	1	2	5
BC Colonization	(+++)	(++)	(+)	(+)
Tissue Penetration	(-)	(+/-)	(+)	(+)
BC Filing	(-)	(+)	(++)	(++)
Tumor Formation	(-)	(+)	(++)	(++)

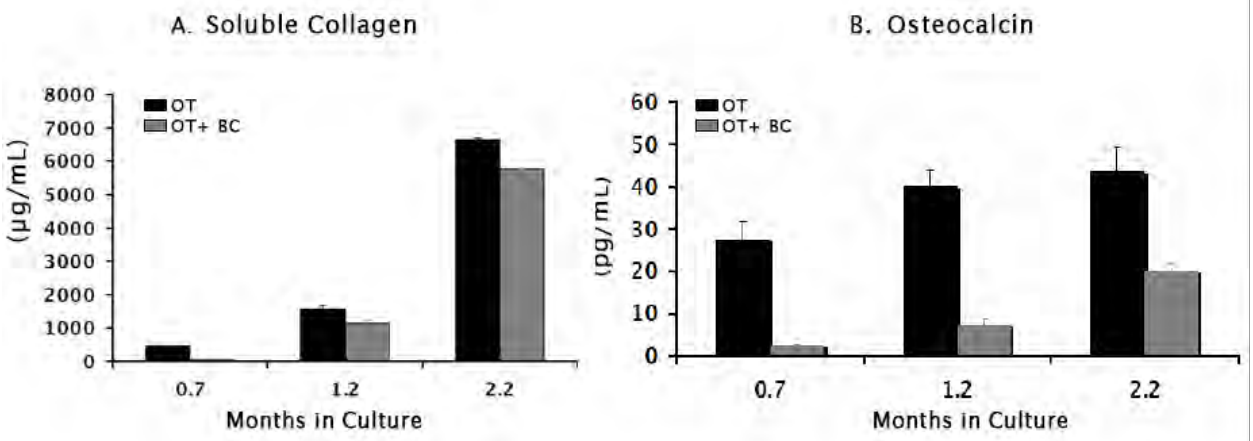
A. Soluble Collagen
OT
OT+ BC
(µg/mL)
8000
7000
6000
5000
4000
3000
2000
1000
0
0.7
1.2
2.2
Months in Culture
B. Osteocalcin
OT
OT+ BC
(pg/mL)
60
50
40
30
20
10
0
0.7
1.2
2.2
Months in Culture

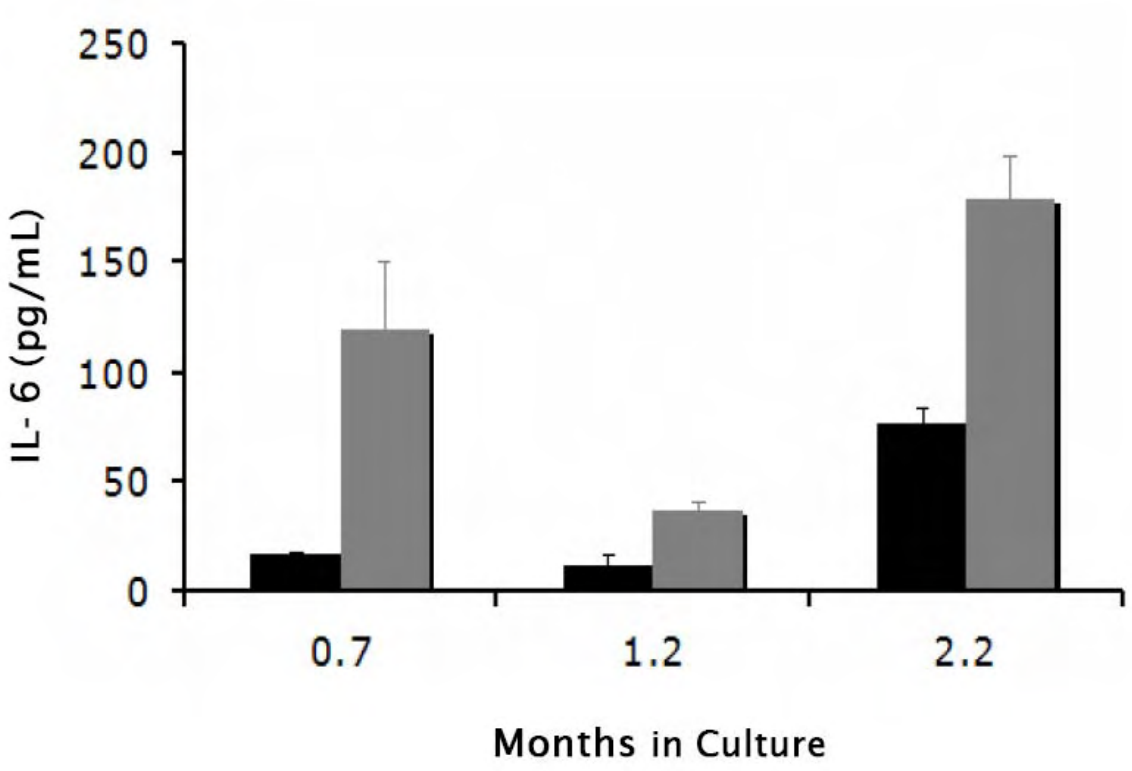

End of Manuscript 1 Draft

Draft
Manuscript 2

Metastatic Breast Cancer Cells Colonize and Penetrate Osteoblast Multi-layers in a 3-D Culture System

A Contribution from the Osteobiology Research Group
The Pennsylvania State University

Laurie A. Shuman[1,4], Venkatesh Krishnan[1,4], Ravi Dhurjati[2], Erwin A. Vogler[2,3,4], and Andrea M. Mastro[1,4]

Departments of [1]Biochemistry and Molecular Biology, [2]Materials Science and Engineering, [3]Bioengineering, and [4]the Huck Institutes of Life Sciences, The Pennsylvania State University, University Park, Pennsylvania 16802.

Running title: 3-D culture of breast cancer cells and osteoblasts

Keywords: breast cancer, osteoblasts, three-dimensional culture, colonization of bone, metastasis

Footnotes: Supported by US Army Medical Research & Materiel Command Breast Cancer Research Program (W81XWH-06-1-0432), Susan G. Komen Breast Cancer Foundation (BCTR104406), Huck Institute Innovation Group, Research Initiation Grant from The Penn State Cancer Institute, and National Foundation for Cancer Research, Center for Metastasis Research, University of Alabama – Birmingham.

Address correspondence to: Andrea M. Mastro, PhD, The Pennsylvania State University, 431 South Frear Building, University Park, PA 16802. Electronic mail: a36@psu.edu

Abstract

Breast cancer frequently metastasizes to bone resulting in the formation of osteolytic lesions. The bone is not repaired even in the presence of drugs, such as bisphosphonates, which inhibit osteoclast activity. The osteoblasts appear to be functionally disabled. In order to examine the interaction of metastatic breast cancer cells with osteoblasts, we have utilized a specialized bioreactor that allows osteoblasts to grow into a multiple-layer, three-dimensional (3-D) mineralizing tissue. We compared co-cultures of metastatic breast cancer cells and osteoblasts grown in the bioreactor to co-cultures carried out using conventional cell culture methods. We find that the breast cancer cells not only attach and grow on the osteoblast tissue in the 3-D system, but form distinct colonies that align along the same axis as the osteoblasts, similar to "Indian filing" seen *in vivo*. Moreover, in this culture system, the breast cancer cells penetrate the osteoblast tissue, a phenomenon not apparent with conventional cell culture methods. Metastatic breast cancer cells interfere with the differentiation of osteoblasts as evidenced by a decrease in production of proteins, such as osteocalcin and collagen. In the presence of the metastatic breast cancer cells the osteoblasts increase production of the inflammatory cytokine, IL-6, which is known to activate osteoclasts. The 3-D culture is superior to 2-D conventional cell culture to study the interaction of metastatic breast cancer cells with osteoblasts. This system should prove useful in manipulating breast cancer cell interactions with osteoblasts in order to determine mechanisms to restore osteoblast function. Word Count: 245

Introduction

Breast cancer preferentially metastasizes to the skeleton and colonizes the ends of long bones, ribs, and vertebrae [1]. Approximately 70% of breast cancer patients who develop metastatic disease show metastasis to the bone. Once metastasis to the bone occurs, the 5-year survival rate declines significantly from 90% to 20% [2,3]. When breast cancer cells enter the bone microenvironment, the balance that normally exists between osteoblasts and osteoclasts is disrupted, and bone loss exceeds repair. Increased osteolysis negatively impacts quality of life due to intense pain, hypercalcemia, and an increased risk for pathologic fractures [3,4,5].

Mechanisms by which breast cancer cells metastasize to and colonize in the skeleton are not well understood partly due to a lack of model systems that accurately mimic the pathogenesis of the disease [28]. However, based on in vitro and in vivo studies, Guise and colleagues propose the “vicious cycle” of bone degradation [6,7]. When breast cancer cells reach the skeleton, they release parathyroid hormone related protein (PTHrP), which indirectly stimulates osteoclasts. Osteoblasts, in the presence of PTHrP, increase expression of receptor activator of nuclear factor kappa B ligand (RANKL), which binds to its receptor, RANK, on pre-osteoclasts to differentiation and activate them to resorb bone. Factors such as transforming growth factor beta (TGF-B), released from the matrix during osteoclast-mediated degradation, stimulate the breast cancer cells to proliferate, producing yet more PTHrP, thus perpetuating the “vicious cycle”. Current therapeutic strategies, such as administration of bisphosphonates (e.g. clodronate), inhibit osteoclast activity and slow lesion formation [8]. However, bone repair is minimal, suggesting that the cancer cells negatively affect osteoblast function.

It has been shown using conventional cell culture methods, i.e. growth of cells in tissue culture plastic, that metastatic breast cancer cells or their conditioned medium inhibit osteoblast differentiation [9], bring about a change in osteoblast morphology [9], increase osteoblast apoptosis [7], and induce production of pro-inflammatory cytokines [10] known to stimulate osteoclast activity.

In this study, a three-dimensional (3-D) cell culture system was used to extend the study of the metastatic bone microenvironment beyond that available in a conventional cell culture model. Cells removed from their native environment to be cultured *in vitro* may retain key phenotypic features, but lose aspects of their differentiated function [11]. The 3-D culture system used in this study allowed osteoblasts to be cultured for extended periods and to generate multiple-cell layer, 3-D mineralizing osteoblastic tissue [12]. This study focuses on the colonization of osteoblast tissue by metastatic breast cancer cells comparing conventional cell culture with a 3-D culture system. Interestingly, in both conventional cell cultures and 3-D cultures, the metastatic breast cancer cells colonized a larger area in less differentiated osteoblasts than in more mature and more differentiated osteoblasts. Here we report that with osteoblasts grown in the 3-D system, the breast cancer cells demonstrated behavior similar to that described *in vivo*. When the osteoid tissue was challenged with metastatic breast cancer cells, we found that the breast cancer cells not only colonized the tissue, but also penetrated it. Moreover, the osteoblasts changed to a spindle shape, and the breast cancer cells aligned in an "Indian Filing" pattern [13,14].

This study validates the 3-D system as a useful *in vitro* model system to study the interaction of breast cancer cells with osteoblasts. With this model the metastatic

breast cancer cells are able to colonize the osteoblasts in a manner similar to that described *in vivo*, i.e. they penetrate the osteoblast matrix and align themselves in an "Indian Filing" pattern.

Materials and Methods

Cell lines. The MC3T3-E1, a murine pre-osteoblast line that can differentiate and mineralize in culture [15], were a gift from Dr. Norman Karin, Pacific Northwest National Laboratories. The cells were maintained in alpha Minimum Essential Medium (αMEM) (Mediatech, Herdon, VA), 10% neonatal FBS (Cansera, Roxdale, Ontario), and penicillin 100 U/ml/streptomycin 100 µg/ml. MC3T-E1 cells were passaged two to three times per week using 0.002% pronase in PBS, and were never used above passage number 20. MDA-MB-231^{-GFP} cells, a human metastatic breast cancer cell line engineered to express green fluorescent protein (GFP) [15,16], were a gift from Dr. Danny Welch, University of Alabama-Birmingham, and were maintained in DMEM, 5% FBS, and penicillin 100 U/ml/streptomycin 100 µg/ml. All cells were grown at 37°C, 5% $CO_{2,}$ in a humidified chamber. Both cell lines were negative for mycoplasma as determined by PCR analysis (Takara Bio Inc., Shiga, Japan).

Conventional cell culture. For experiments, MC3T3-E1 cells were plated at 10^4 cells/cm^2 in differentiation medium [αMEM, 10% FBS, penicillin 100 U/ml/streptomycin 100 µg/ml, 50 µg/ml ascorbic acid, and 10 mM β-glycerophosphate (Sigma-Aldrich Corp.,St. Louis, MO)], and grown for the indicated number of days in 35-mm polystyrene cell culture plates (Sarstedt Inc., Newton, NC). MDA-MB-231^{-GFP} metastatic breast cancer cells were added to the osteoblasts at various ratios of breast cancer

cells (BC) to osteoblasts (OB) as indicated in each experiment. Co-cultures were carried out for the indicated number of days. The co-culture systems were maintained in MC3T3-E1 differentiation medium. At the end of the designated co-culture periods, images were taken with a fluorescence microscope (Leitz, Diavert). Culture media were collected to measure protein secretion by osteoblasts using ELISA (murine specific Mouse Bone Panel 2B, LINCOplex™, Millipore, Missouri, USA). The cells were washed once with PBS prior to RNA extraction (RNeasy, Qiagen, Valencia, CA) or before staining with Wrights-Giemsa to view morphology.

Bioreactor culture system. A specialized, compartmentalized bioreactor was used to culture osteoblasts [12]. The bioreactor design is based on the principle of simultaneous growth and dialysis, which allows for a stable peri-cellular environment. Osteoblasts were plated at 10^4 cells / cm^2 in the chamber of 25 cm^2 in growth medium. After 4-7 days when the cultures appeared to be confluent, the medium was changed to differentiation medium. The osteoblasts were allowed to grow in the bioreactor for 15, 30, or 60 days prior to the addition of MDA-MB-231^{-GFP} cells. The breast cancer cells (BC) were added to the osteoblast (OB) cultures at ratios of 1:10, 1:100, or 1:1000 based on previous determination of the number of osteoblasts present at each time. After 7 days of co-culture, the bioreactors were dismantled and the substratum with adherent tissue was cut into pieces for various assays. The media from both the upper chamber and lower chamber were collected. Osteocalcin (OCN) and interleukin-6 (IL-6) secreted from the osteoblasts were determined using ELISA (murine specific Mouse Bone Panel 2B, LINCOplex™, Millipore, Missouri, USA).

Light / Fluorescence Microscopy. At the end of the co-culture period, light and fluorescence microscope images of the cells in the 35-mm polystyrene dishes were obtained using a Leitz Diavert microscope and a NIKON CoolPix 8400 digital camera. Three random fields were imaged from each culture dish. Images were saved as JPEGs and the ImageJ program (NIH) was used to calculate the percent area of breast cancer cell colonization based on the fluorescent images.

Confocal microscopy. For live cell imaging, osteoblasts were stained with 10μM Cell Tracker Orange™ (Invitrogen Corporation, Carlsbad, CA) prior to the addition of MDA-MB-231^{-GFP} breast cancer cells. This concentration was determined not to affect cell viability (data not shown). Images were collected by sequential scans using the Olympus FV300 laser scanning confocal microscope. The Z-stacks were 3D-reconstructed using the AutoQuant v9.3 software. The cell layers were determined visually by counting and following the sub-volumes of cells in the 3D-reconstructed Z-stack images. At the end of the co-culture period, the tissue was fixed in 2.5% glutaraldehyde in cacodylate buffer and stained for actin filaments with 33nM AlexaFlour phalloidin-568™ stain (Molecular Probes, Invitrogen Corporation, Carlsbad, CA) for further morphological analysis by confocal imaging.

Transmission Electron Microscopy (TEM). Cultures were washed once with PBS, fixed overnight with 2.5% glutaraldehyde in cacodylate buffer at 4°C followed by a secondary fixation with 1% osmium tetroxide in cacodylate buffer for 1h at room temperature prior to en bloc staining with 2% aqueous uranyl acetate for 1h. Dehydration was preformed using a graded series of ethanol concentrations, followed

by impregnation and embedding in Spurr's resin. Ultra-thin sections were cut with a **diamond** knife (Diatome Ultra 45) on a microtome (Ultracut UCT, Leica), placed on uncoated copper grids, and stained with 0.2% aqueous uranyl acetate and 0.2% lead citrate. The cross sections were examined using TEM (JEM 1200 EXIL, JEOL), and images were collected using an attached high-resolution camera (Tietz F224, Gaunting).

Reverse transcription polymerase chain reaction (RT-PCR). MC3T3-E1 were cultured in standard tissue culture plates or in the bioreactor for various times. MC3T3-E1 cells were washed one time with PBS, and RNA was isolated using Rneasy Kit (Qiagen). RNA purity was determined by the A260 / A280 ratio; all samples had a ratio > 1.8. CDNA was generated from 1 μg RNA using RETROscript kit (Ambion). The sequences of the PCR primer pairs used for amplification are listed in Table 1. PCR was carried out on a thermocycler [DetaCylcer 1™ System (Ericomp)]. PCR reactions were run on a 2% agarose gel, stained with ethidium bromide and imaged under UV illumination (Kodak).

Collagen synthesis. Soluble collagen (indicative of collagen synthesis) was quantified using The Sircol™ Assay (Biocolor Ltd., Newtonabbey, North Ireland). Prior to running the assay as per the manufacturers protocol, the collagen was extracted / precipitated from cell culture supernatants by addition of NaCl (4M final concentration). Supernatants were centrifuged and the collagen pellet was resuspended in 0.5M acetic acid.

Results

The rate of breast cancer cell colonization depends upon the stage of osteoblast differentiation. To determine if the stage of osteoblast differentiation influenced breast cancer growth, MC3T3-E1 osteoblasts were grown to early, middle, and late stages of differentiation (4, 14, and 24 days respectively) in polystyrene cell culture dishes (Sarstedt Inc., Newton, NC) before being co-cultured with MDA-MB-231^{-GFP} metastatic breast cancer cells. The co-cultures were carried out for 7 days. Under all stages of osteoblast differentiation, the breast cancer cells attached, grew, and formed colonies. Figures 1A (left column) and 1D (top) are images of osteoblasts grown in differentiation medium (containing osteoinductive agents) for 4 days prior to the addition of breast cancer cells. As the osteoblasts reached confluence they began to acquire a cuboidal morphology (Figure 1D-top,left). These osteoblasts were considered to be in the early stages of differentiation because they did not yet express osteopontin, osteonectin and osteocalcin (Figure 4A). However, these early differentiation osteoblasts had started to express type I collagen, a main component of the extracellular matrix that gives bone its strength and elasticity (Figure 4A).

MDA-MB-231^{-GFP} breast cancer cells were added to these day 4 cultures of MC3T3-E1 osteoblasts at three different ratios of breast cancer cells (BC) to osteoblasts (OB), (1 BC : 10 OB, 1 BC : 100 OB, or 1 BC : 1,000 OB). At all three ratios the cancer cells attached to the osteoblasts within one hour (data not shown), proliferated, and formed colonies apparently on top of the osteoblasts within 7 days of co-culture (Figure 1A-left column). At seven days approximately 31% of the area was covered by breast cancer cells from the initial inoculation of 1:10, 14% at 1:100, and 7% at 1:1,000.

By 11 days in culture, the osteoblasts already expressed more differentiation proteins (see Figure 4A). They also stained positive for alkaline phosphatase, and produced hydroxyapetite crystals indicated by von kossa staining (data not shown). When 14 day-old osteoblasts were challenged with metastatic breast cancer cells, the breast cancer cells attached and colonized the osteoblast cultures. However, the percent area of the 14 day-old osteoblasts covered by the breast cancer cells at the 1:10 ratio was dramatically reduced (8.1%) compared to that seen with the 4 day-old osteoblasts (31.0%) (Figure 1A-middle column). The area colonized was lower also in the cultures with breast cancer cells at 1:100 and 1:1,000 OB, as well.

After 24 days in differentiation medium, the osteoblasts produced abundant extracellular matrix, showed increased alkaline phosphatase activity, and enhanced mineralization. Interestingly, when the 24 day-old osteoblasts were co-cultured with breast cancer cells for 7 days, the cancer cells only formed small colonies (Figure 1A-right column). Only 5% of the osteoblast culture was covered by cancer cells in the 1:10 condition (Figure 1A), and only 0.8% at the 1:1,000 ratio.

To investigate if the metastatic breast cancer cells would eventually colonize the more mature, 24 day-old osteoblasts over a longer co-culture period, breast cancer cells were added to 24 day-old osteoblasts at a ratio of 1 BC : 10 OB and observed for 14 days of co-culture (Figure 1B). Images were taken after 1, 3, 7, and 14 days in co-culture. By 14 days in co-culture the breast cancer cells colonized 33% of the area of the 24 day-old osteoblast culture equivalent to that seen in the 7 day co-cultures of 4 day-old osteoblasts (31%). Therefore, although the metastatic breast cancer cells

showed delayed colonization in the presence of more mature osteoblasts, they eventually grew.

In summary, in all three stages of osteoblast differentiation, the breast cancer cells colonized a greater area of the osteoblast culture when added at the 1 BC : 10 OB ratio versus the 1BC : 1,000OB ratio (Figure 1C). However, the rate of colonization was greatest in the 4 day-old osteoblast cultures. Eventually, the cancer cells grown on the more mature osteoblasts reached the same level of colonization as seen on the less differentiated osteoblasts.

Cancer cells affected osteoblast morphology. Previously, we reported that conditioned medium collected from human metastatic MDA-MB-231 breast cancer cells caused MC3T3-E1 osteoblasts to undergo a change in morphology [9]. After exposure to metastatic breast cancer conditioned medium, the osteoblasts appeared long and spindly rather than cuboidal, more similar to a fibroblast. In order to determine if this change in shape occurred in co-culture, the co-cultures of MC3T3-E1 and MDA-MB-231^{-GFP} were stained with Wrights-Giemsa at the termination of the 7 day co-culture period. The osteoblasts stained pink, while the cancer cells were appeared as dark purple clusters (Figure 1D). In co-cultures where osteoblasts were 4 days old prior to the addition of the breast cancer cells, the entire osteoblast culture showed a dramatic change in morphology from cuboidal (Figure 1D, Day 4 left column) to spindle-shaped and striated (Figure 1D, Day 4 right column). This culture-wide change was not evident when the breast cancer cells were added to 14 or 24 day-old osteoblasts. In both of these cases, only the osteoblasts bordering the breast cancer colonies showed altered morphology. The osteoblast monolayer directly bordering the breast cancer colonies

became thinner, and the cells became more striated and appeared to be surrounding the breast cancer colonies (Figure 1D, inserts).

Metastatic breast cancer cells colonize and penetrate osteoblasts when co-cultured in a bioreactor. Once the MC3T3-E1 cells were grown longer than about 30 days in standard cell culture, they began to detach from the sides of the plate. The cultures grew mostly as a monolayer, or at most, formed 2 cell layers. However, MC3T3-E1 cultured in the bioreactor can be grown for many months [10]. During this time they form several layers of cells in a partially mineralized matrix. We asked how MDA-MB-231^{-GFP} cells interacted with the osteoblast tissue under these conditions. MC3T3-E1 osteoblasts grown in the bioreactor for 15, 30, or 60 days expressed osteoblast differentiation genes including osteocalcin, osteonectin, and type I collagen (Figure 4A). To enable visualization of the osteoblast morphology by confocal microscopy, the osteoblasts were fixed and stained with phalloidin, which binds to actin filaments. Up to 60 days in culture in the bioreactor, the osteoblasts underwent a phenotypic change from a monolayer of striated cells to multi-layers of tissue containing cuboidal osteoblasts (Figure 2A). Osteoblasts grown for 15 days produced abundant collagen, a trait of maturing osteoblasts, as seen by transmission electron microscopy (Figure 3F). The extracellular matrix was apparent in the older cultures as well. Osteoblasts grown for 15, 30, or 60 days in the bioreactor produced 28, 40, and 44 μg/mL of soluble collagen, respectively.

When osteoblasts grown in the 3-D culture system for 15, 30, or 60 days were challenged with MDA-MB-231^{-GFP} metastatic breast cancer cells at ratios of 1 BC: 10 OB or 1 BC: 100 OB, the cancer cells and the osteoblasts exhibited both similarities and

differences to those observed in co-cultures carried out in plastic. MC3T3-E1 were stained with Cell Tracker Orange™ prior to the addition of GFP expressing metastatic breast cancer cells (MDA-MB-231^{-GFP}) in order to distinguish osteoblasts (red) from breast cancer cells (green) using confocal fluorescence microscopy. Z-stack images were taken in 1 μm increments and compiled to generate 3-D reconstructions (Figure 2B). Breast cancer cells added to 15 day-old osteoblasts at a ratio of 1 BC : 10 OB formed many coinciding colonies (Figure 2B, left column, top). However, as osteoblasts matured from 15 days in culture to 60 days in culture, breast cancer cells formed fewer interconnected colonies. When osteoblasts were challenged with fewer cancer cells (Figure 2B, right column), recapitulating micrometastases, the breast cancer cells formed distinct, large colonies dispersed within the osteoblast tissue. The more mature the osteoblast tissue, the smaller and fewer the breast cancer colonies. This delayed rate of breast cancer colonization was observed in both the 1 BC : 10 OB ratio and the 1 BC : 100 OB ratio. In addition, the osteoblasts directly surrounding the breast cancer colonies appeared less cuboidal (Figure 2A) and more striated (Figure 2B). Importantly, when comparing 14 day-old osteoblasts co-cultured in conventional cell culture (Figure 1A, middle) to 15 day-old osteoblasts co-cultured in the 3-D system (Figure 2B, top), it was apparent that the osteoid tissue was a more hospitable environment for breast cancer colonization. Breast cancer cells were able to form more and larger colonies in the 3-D co-culture system than in conventional cell culture. This growth pattern was most likely due to the accumulation of growth factors and cytokines from both osteoblasts and breast cancer cells in the growth chamber of the bioreactor. These

factors are normally removed with medium changes from cells grown in conventional culture.

TEM analysis of the interaction of breast cancer cells with osteoblasts in the bioreactor and in conventional cell culture. The osteoblasts grown in the bioreactor formed multi-layers of bone-like tissue. The human metastatic breast cancer cells were able to penetrate the 15, 30, or 60 day-old osteoblast tissue (supplemental data and Figure 3E). This behavior was not observed in standard cell culture dishes (Figure 3D). TEM analysis (Figure 3A) and confocal Z-stack images of Cell Tracker Orange™ - stained osteoblasts (Figure 3G) verified that osteoblasts grown in standard cell culture dishes achieve one or at most two cell layers.

The interaction of the breast cancer cells with the osteoblasts was observed by TEM after 1 day, 3 days, and 6 days of co-culture in standard cell culture dishes (Figure 3 B, C, and D respectively). Cancer cells initially spread on top of the osteoblast culture (Figure 3B, BC). After 3 days the breast cancer cells eventually formed large colonies on the upper surface of the osteoblast culture (Figure 3D), and became more rounded (Figure 3C). The breast cancer cells were never observed to penetrate the osteoblast layer(s). Co-cultures of osteoblasts with metastatic breast cancer cells in the 3-D culture system indicated that breast cancer cells penetrated the osteoblast layers (Figure 3E), and attach to the substratum (indicated by arrow heads). In addition, when breast cancer cells were co-cultured with osteoblasts in the bioreactor, the cancer cells aligned themselves along the same axis as the osteoblasts in organized rows (Figure 3 H,I). This phenomenon appeared to be similar to “Indian Filing” as described by

pathologists [13, 14], and was not seen in co-cultures grown in plastic cell culture plates.

Osteoblasts co-cultured with metastatic breast cancer cells in 2-D and 3-D systems exhibited decreased collagen deposition. TEM images of 15 day-old osteoblasts show pronounced collagen fibers (Figure 3,A). In as little as 24 hours in co-culture, the collagen structure appeared speckled in TEM images rather than fibrous indicative of collagen degradation (Figure 3, B). After 7 days in 3-D co-culture, much of the abundant collagen produced by osteoblasts (Figure 3F) was no longer detected (Figure 3E). Thus the extent to which osteoblasts are affected by breast cancer cells is not fully captured in 2D conventional cell culture partly because the osteoblasts cannot generate multi-layered tissue similar to bone, and cytokines and growth factors secreted by both osteoblasts and breast cancer cells are removed with routine medium changes.

Osteoblasts co-cultured with breast cancer cells secrete less osteocalcin and increase production of interleukin-6. We previously reported that osteoblasts increased the secretion of inflammatory cytokines, i.e. IL-6, MCP-1, MIP-2, when exposed to conditioned medium collected from metastatic breast cancer cells [10].

Interleukin-6 (IL-6) was used as an indicator of this response. It was produced by osteoblasts in greater amounts at each stage of differentiation when co-cultured with human metastatic breast cancer cells compared to cultures of osteoblasts alone (Figure 4C). An increase in the production of IL-6 by murine osteoblasts was detected in cultures with human breast cancer cells in both conventional cell culture and in the 3-D system using a species-specific multiplex cytokine kit (LincoPlex, Mouse Bone Panel 2B). We also found that in the presence of breast cancer cells the osteoblasts, led to

decreased secretion of osteocalcin, a noncollagenous protein involved in mineralization and calcium ion homeostasis (Figure 4B). Leptin and secreted RANKL were not detected in osteoblast cultures or co-cultures.

Discussion

While there were similarities in the response of osteoblasts to breast cancer cells in both 2-D and 3-D systems, there were major differences also. In both systems there was a change in osteoblast morphology near the cancer cell – osteoblast border, increased production of the pro-inflammatory cytokine, IL-6, and decreased secretion of osteocalcin (Table 2). When metastatic breast cancer cells were introduced into the osteoblast microenvironment in conventional cell culture dishes, the cancer cells attached, proliferated, and formed distinct colonies on top of the osteoblast monolayer. However, culture in the 3-D system allowed osteoblasts to differentiate and produce a multi-layered bone-like tissue, which metastatic breast cancer cells penetrated and colonized in a unique “Indian Filing” pattern similar to the pathology of invasive carcinomas [13,14].

We noted that the collagen synthesis as detected by production of soluble collagen, was affected in co-cultures. The amount of soluble collagen produced by osteoblasts, measured by the Sircol™ assay, decreased after seven days in co-culture with metastatic breast cancer cells from 28 μg/mL to 3μg/mL in 15 day-old cultures, from 40μg/mL to 7 μg/mL in 30 day-old cultures, and from 44 μg/mL to 20 μg/mL in 60 day-old cultures. Collagen is degraded by a family of proteases, matrix metalloproteinases (MMPs) [18]. There are membrane-type metalloproteinases (MT-MMPs) and secreted MMPs, which are classified into groups, such as collagenases,

gelatinases, and stromelysins, based on substate specificity. MMPs capable of degrading collagen include MMP-1,2,8,9,13,14. It has been shown that more invasive breast cancer cells, such as MDA-MB-231, have high levels of these active MMPs [17,18,19]. Others have reported an increased expression of MMP-13 in MC3T3-E1 cells correlating to their increased stage of differentiation [30,31]. MDA-MB-231 breast cancer cells are highly invasive and metastatic, and exhibit both protease-dependent and protease-independent mechanisms of migration [13,19]. When migrating through 3-D matrices, tube-like tracks are visible from local protease-mediated degradation of the extracellular matrix. However, treatment with pharmalogical inhibitors to MMPs, serine proteases, and cathepsins does not inhibit cell migration, indicating a protease-independent mechanism for tumor cell migration [25]. This protease-independent migration is referred to as an “amoeboid” form of migration, whereby tumor cells squeeze through spaces in the extracellular matrix [13,25]. We see both collagen degradation in the presence of breast cancer cells and the extension of long processes from the breast cancer cells into the osteoblast tissue (see Dhurjati et al, manuscript submitted).

Conventional cell culture requires frequent medium changes, which disturbs cells and removes cytokines, growth factors, and proteases secreted into the microenvironment. The 3-D bioreactor culture system requires only infrequent medium changes, allowing various growth factors and cytokines to accumulate. This accumulation of factors in the microenvironment is an important feature of the 3-D culture system enabling the cells to respond in a more *in vivo* like fashion. Griffith and Swartz summarize the importance a 3-D environment has on the cues cells send to and

receive from each other due to mechanical inputs and the binding of cell adhesion molecules [29]. Additionally, 3-D environments have a concentration gradient created from the competition of diffusion and convection of the factors consumed and produced by the cells, which impacts the tissue physiology [29].

The development of 3-D *in vitro* models is expanding our understanding of cancer research [20,21]. 3-D *in vitro* culture systems enable cells (tumor and non-tumor) to grow and organize in a more biologically relevant manner, thus enhancing our ability to observe and manipulate cancer progression. Tumor cells grown in 3-D culture systems exhibit pathway activities and receptor expression more similar to *in vivo* tumor specimens than do tumor cells grown in conventional cell culture [20]. For example, 3-D cultures helped in the determination of several mechanisms that glandular epithelial tumors use to fill the lumen during tumorogenesis, including disregulation of both proliferation and apoptosis or activation of oncoproteins, such as ERBB2, CSF1R, SRC, and IGF1R [20,21,22,23,24,25]. This process could not be studied in conventional cell culture. Most importantly the cell-cell contact between tumor and non-tumor cells can be monitored in a 3-D culture system unlike *in vivo* systems, which require specialized microscopy or sacrifice of the animal to examine cell interactions. In addition, 3-D model systems that more accurately mimic *in vivo* phenotypes, such as the 3-D cell perfusion-culture system in microfluidic channels, are being designed to advance drug toxicity, metabolism, and stem cell differentiation studies [27].

In conclusion, the 3-D *in vitro* bioreactor culture system used in this study was superior to conventional cell culture for observing the interaction of metastatic breast cancer cells with osteoblast tissue. Cells cultured in this system were able to be

monitored over time and exhibited characteristics observed *in vivo* that have not been seen *in vitro* using conventional cell culture methods. The bioreactor not only permitted cancer cell growth and colonization, but also enabled the breast cancer cells to align in a distinct filing fashion and penetrate the osteoblast tissue.

Acknowledgements

We would like to acknowledge Donna M. Sosnoski for help with the PCR experiments, Elaine Kunze, Nicole Bem, and Susan Magargee of the Huck Institutes of the Life Sciences Cytometry Facility for help with confocal microscopy, and Missy Hazen of the Electron Microscopy Core Facility for help with transmission electron microscopy.

References

1. Rubens, R.D. and Mundy G.R. Cancer and the skeleton. In: Rubens, R.D. and Mundy, G.R., editors. London: Martin Dunitz, 2000. p. 892-893.
2. Roodman, GD. "Biology of osteoclast activation in cancer." J Clin. Oncol. 19:2001. 3562-3571.
3. Coleman, R. Skeletal complications of malignancy. Cancer 1997; 80: 1588-1594.
4. Lipton, A., Theriault, R.L., Hortobagvi, G.N., et al. Pamidronate prevents skeletal complications and is effective palliative treatment in women with breast carcinoma and osteolytic bone metastases: Long term follow-up of two randomized, placebo-controlled trials. Cancer 2000; 88: 1082-109
5. Ural, A.U., Avcu, F., Baran, Y. Bisphosphonate treatment and radiotherapy in metastatic breast cancer. Medical Oncology 2008; epub ahead of print January 18, 2008.
6. Guise TA. 2000. Molecular mechanisms of osteolytic bone metastases. Cancer; 88: 2892–2898.
7. Mastro, A.,Gay, C.V., Welch, D.R., et al. Breast Cancer Cells Induce Osteoblast Apoptosis: A Possible Contributor to Bone Degradation. Journal of Cellular Biochemistry 2004; 91: 265-276.
8. Santini, D., Gentilucci, U.V., Vincenzi, B., et al. The antineoplastic role of bisphosphonates: from basic researh to clinical evidence. Annals of Oncology 2003; 14: 1468-1476.
9. Mercer, R.R., Miyasaka, C. and Mastro, A.M. "Metastatic breast cancer cells suppress osteoblast adhesion and differentiation. Clinical Experimental Metastasis 2004; 21: 427-435.

10. Kinder, M., Chrislock, E., Bussard, K.M., Shuman, L.A., and Mastro, A.M. Metastatic Breast Cancer Induces An Osteoblast Inflammatory Response. Experimental Cell Research 2007; 314: 173-183.
11. Karin, N.J. and Farach-Carson, M.C. In vitro regulation of osteoblast activity. In: Bronner, F. and Farach-Carson, M.C., editors. London: Springer; 2004. p.18-43. Bone Formation.
12. Dhurjati, R., Liu, X., Gay, C.V., Mastro, A.M., and Vogler, E.A. Extended-term culture of bone cells in a compartmentalized bioreactor. Tissue Engineering 2006; 12 (11): 3045-3054.
13. Friedl, P. and Wolf, K. Tumour-cell invasion and migration: diversity and escape mechanisms. Nature Rev. Cancer 2003; 3: 362-374.
14. Adelson, R.T., DeFatta, R.J., Miles, B.A., Hoblitt, S.L., and Ducic, Y. Metastatic breast cancer of the oral cavity. American Journal of Otolaryngology-Head and Neck Medicine and Surgery 2005; 26: 279-281.
15. Quarles, L., Yohay, D., Lever, L., Caton, R., and Wenstrup, R. Distinct proliferative and differentiated stages of murine MC3T3-E1 in culture: an in vitro model of osteoblast development. Journal of Bone and Mineral Research 1992; 7 (6): 683-692.
16. Cailleau, R., Olive, M., and Crueiger, Q. Long term human breast carcinoma cell lines of metastatic origin: preliminary characterization. *In Vitro* 1978; 14: 911-915.
20
17. David, D.B., Reznick, A.Z., and Livne, E. Exposure to pro-inflammatory cytokines upregulates MMP-9 synthesis by mesenchymal stell cells-derived osteoprogenitors. Histochemistry and Cell Biology 2008; published online February 15, 2008.
18. Tester, A., Ruangpanit, N., Anderson, R.L., and Thompson, E.W. MMP-9 secretion and MMP-2 activation distinguish invasive and metastatic sublines of a mouse mammary carcinoma system showing epithelial-mesenchymal transition traits. Clinical & Experimental Metastasis 2001; 18: 553-560.
19. Yu, M., Sato, H., Seiki, M., Spiegel, S., and Thompson, E.W. Elevated cyclic AMP suppresses ConA-induced MT1-MMP expression in MDA-MB-231 human breast cancer cells. Clinical Experimental Metastasis 1998; 16: 185-191.
20. Schmeichel, K.L., and Bissell, M.J. Modeling tissue-specific signaling and organ function in three dimensions. Journal of Cell Science 2003; 116 (12): 2377-2388.
21. Debnath, J., and Brugge, J. Modelling gladular epithelial cancers in three-dimensional cultures. Nature Reviews Cancer 2005; 5: 675-687.
22. Reginato, M.J., Mills, K.R., Becker, E.B.E., et al. BIM regulation of lumen formation in cultured mammary epithelial acini is targeted by oncogenes. Molecular Cellular Biology 2005; 25: 4591-4601.
23. Muthuswamy, S.K., Li, D., Lelievre, S., Bissell, M.J., and Brugge, J.S. ERBB2, not ERBB1, reinitiates proliferation and induces luminal repopulation in epithelial acini. Nature Cell Biology 2001; 3: 785-792.
24. Wrobel, C.N., Debnath, J., Lin, E., Beausoleil, S., Roussel, M.F., Brugge, J.S. Autocrine CSF-1R activation promotes SRC-dependent disruption of mammary epithelial architecture. Journal Cellular Biology 2004; 165: 263-273.

25. Kacinski, B.M., Scata, K.A., Carter, D., et al. FMS (CSF1 receptor) and CSF-1 transcripts and protein are expressed by human breast carcinomas *in vivo* and *in vitro*. Oncogene 1991; 6: 941-952.
26. Cailleau, R., Olive, M., and Crueiger, Q. Long term human breast carcinoma cell lines of metastatic origin: preliminary characterization. In Vitro 1978; 14: 911-915.
27. Toh, Y., Zhang, C., Khong, Y.M., et al. A novel 3D mammalian cell perfusion-culture system in microfluidic channels. Lab Chip 2007; 7: 302-309.
28. Phadke, P.A., Mercer, R.R., Harms, J.F., et al. Kinetics of metastatic breast cancer cell trafficking in bone. Clinical Cancer Research 2006; 12 (5): 1431-1440.
29. Griffith, L.G., and Swartz, M.A. Capturing complex 3D tissue physiology in vitro. Nature Reviews Molecular Cell Biology 2006; 7: 211-224.
30. Mizutani, A., Sugiyama, I., Kuno, E., Matsunaga, S., and Tsukagoshi, N. Espression of matrix metalloproteinases during ascorbate-induced differentiation of osteoblastic MC3T3-E1 cells. Journal of Bone and Mineral Research 2001; 16 (11): 2043 – 2049.
31. Zaragoza, C., Lopez-Rivera, E., Garcia-Rama, C., et al. Cbfa-1 mediates nitric oxide regulation of MMP-13 in osteoblasts. Journal of Cell Science 2006; 119: 1896 – 1902.

Table 1. Primer sequences and experimental conditions for RT-PCR

Gene	Primers (F=Forward; R=Reverse)	Annealing Temperature (°C)	Cycles	Amplicon Size (bp)
Osteocalcin	F: 5'- CAA GTC CCA CAC AGC AGC TT- 3' R: 5'- AAA GCC GAG CTG CCA GAG TT- 3'	55	23	370
Osteonectin	F: 5'- CTG CCT GCC TGT GCC GAG AGT TCC- 3' R: 5'- CCA GCC TCC AGG CGC TTC TCA TTC- 3'	55	17	653
Type I Collagen	F: 5'- TCT CCA CTC TTC TAG TTC CT- 3' R: 5'- TTG GGT CAT TTC CAC ATG- 3'	55	16	269
MMP-13	F: 5'- GAT GAC CTG TCT GAG GAA G- 3' R: 5'- ATC AGA CCA GAC CTT GAA G- 3'	58	21	357
β-Actin	F: 5'- CGT GGG CCG CCC TAG GCA- 3' R: 5'- TTG GCC TTA GGG TTC AGG- 3'	62	20	242

Table 2. Comparison between breast cancer and osteoblast interactions in 2D and 3D culture

	Experimental Parameter	Culture Method	
A	**Osteoblasts**	**2D**	**3D**
	Proliferation	++	+++
	Maturation	++	+++
	Mineralization	++	+++

B		Age of OB (Days)					
	Co-Culture at BC:OB =1:10	4	14	24	15	30	60
	Change in OB Morphology	++	+	+	+	++	++
	Breast Cancer Colonization	+++	++	+	+++	++	+
	Tissue Penetration	-	-	-	-	(-/+)	+
	Breast Cancer Filing	-	-	-	-	+	++
	Collagen Breakdown	-	+	+	(-/+)	+	++
	IL-6 Increase	(-/+)	++	+	+	++	++

Figure Legends

Figure 1. Co-culture of MC3T3-E1 osteoblasts with metastatic breast cancer cells, MDA-MB-231^{-GFP}, in conventional cell culture. At various stages of osteoblast growth / differentiation (day 4, 14, or 24) breast cancer cells (BC) were added to osteoblasts (OB), at one of three ratios of BC to OB (1:10, 1:100, and 1:1000). Co-culture was carried out for 7 days. (A) The effect of increasing osteoblast differentiation state and breast cancer to osteoblast ratios on the colonization of the cultures by the cancer cells after 7 days. Shown are the fluorescence microscopic images of co-cultures. Values indicate percentage of culture area occupied by the breast cancer cells as calculated by the Image J analysis tool (NIH). Three fields were viewed and analyzed at each point (5,000X). (B) Colonization of differentiated (day 24) osteoblasts by the cancer cells at various days of co-culture up to 14 days. Breast cancer cells were added at a ratio of 1 BC:10 OB to 24-day cultures of MC3T3-E1 osteoblasts. Co-cultures were imaged after 1, 3, 7, and 14 days. Percent colonization was calculated as described in A. (C) Graphical representation of breast cancer colonization of osteoblasts at various stages of osteoblast differentiation. Plotted is the percent colonization (A) versus the days in culture. (D) Wrights-Giemsa stained co-cultures established as described in A. At the indicated times, medium was removed from the co-cultures, the cells were washed with PBS, fixed in cold absolute methyl alcohol and stained with Wrights-Giemsa (Fisher Diagnostics LeukoStat Stain Kit). Shown are images of osteoblasts alone (OB) or of 7 day co-cultures of breast cancer cells and osteoblasts where the cancer cells were added to the osteoblasts at a ratio of 1 BC : 10 OB (OB+BC). The osteoblasts appear mostly pink with dark nuclei while the cancer cells appear as dark clusters. Inserts

(arrow) represent 40X magnification of boxed in area. Images were collected using a light microscope. Magnification bars indicate 100 μm on all images.

Figure 2. Maturation of MC3T3-E1 in the bioreactor (A) and co-culture of MDA-MB-231^{GFP} cells with osteoblasts in the bioreactor (B). MC3T3-E1 were cultured in the bioreactor as described in the materials and methods section for up to 2 months. Shown are confocal images of osteoblasts fixed and stained with Phalloidin Alexa Fluor™ 568. (A) The cells underwent a phenotypic change from a pre-osteoblast monolayer of spindle-shaped cells to cuboidal osteoblasts in a multilayered tissue. Scale bar represents 50μm. (B) MC3T3-E1 (OB) were cultured in the bioreactor for 15, 30, or 60 days before addition of MDA-MB-231^{GFP} (BC) at ratios of BC:OB, 1:10 or 1:100. After 7 days in co-culture, the cells were fixed and stained with phalloidin Alexa Fluor™ 568 and images were collected using a confocal microscope. Shown are 3D reconstructed Z-stacks of the co-cultured tissue. Scale bar represents 100 μm.

Figure 3. Transmission electron microscopy (TEM) and confocal analysis of MC3T3-E1 osteoblasts grown alone or in co-culture with metastatic breast cancer cells, MDA-MB-231^{-GFP}, in conventional polystyrene cell culture plates (A-D, G) or in the bioreactor (E,F,H,I). Osteoblasts were grown alone for 15 days in tissue culture plates prior to the addition of metastatic breast cancer cells at a ratio of 1 BC : 3 OB. Co-cultures were carried out for 1 day, 3 days, or 6 days before being processed and sectioned for TEM analysis. Shown are TEM images of osteoblasts alone (A), in co-culture with breast cancer cells for 1 day (B), 3 days (C), or 6 days (D). Magnification bars indicate 1μm.

Shown in (E) is a TEM image of 60 day- old osteoblasts co-cultured with MDA-MB-231^{GFP} breast cancer cells for 10 days. Magnification bar indicates 5μm. Arrows indicate substratum of the bioreactor. (F) TEM section of a 15 day-old osteoblasts showing abundant collagen fibers between the cell layers. Scale bar indicates 5μm. (G) Confocal image of 15 day-old osteoblasts stained with Cell Tracker Orange™. Shown below is the xz plane cross-section of the osteoblast culture and to the right is the yz plane cross-section of the osteoblast culture used to determine the depth of the osteoblast culture. Magnification bar represents 50 microns. (H) 3-D reconstruction of confocal images of 60 day-old osteoblasts co-cultured with GFP-expressing breast cancer cells for 5 days. Osteoblasts were stained with Cell Tracker Orange™ (red) while the breast cancer cells fluoresce green. Magnification bars represent 100 μm. (I) Confocal image of the same culture shown in (H), but after 7 days of co-culture. Magnification bars represent 100 μm.

Figure 4. Expression of osteoblast differentiation genes and IL-6 over time. MC3T3-E1 cells were cultured in a bioreactor or in standard cell culture dishes as described in the materials and methods section. At indicated times (22, 30, 60 days for the bioreactor samples and 5, 7, 11, and 21 days for cell culture samples), the cells were harvested and RNA isolated (RNeasy kit, Qiagen).

RT-PCR was carried out using the primers listed in Table 1. Ethidium bromide stained bands were quantitated using Imagequant (Molecular Dynamics) and normalized to β-actin. Shown are representative amplicons bands (A). Quantitative plot of secreted

osteocalcin protein from osteoblasts of various ages compared to osteoblasts cultured with breast cancer cells for a co-culture period of 7 days in standard cell culture (B-left) or in the bioreactor (B-right). Protein levels of the pro-inflammatory cytokine, IL-6, secreted by the osteoblasts in the presence and absence of metastatic breast cancer cells grown in standard cell culture (C-left) or in the bioreactor (C-right). IL-6 and osteocalcin protein levels were quantified using a mouse specific ELISA assay from Millipore (LINCOplex™ Mouse Bone Panel 2B).

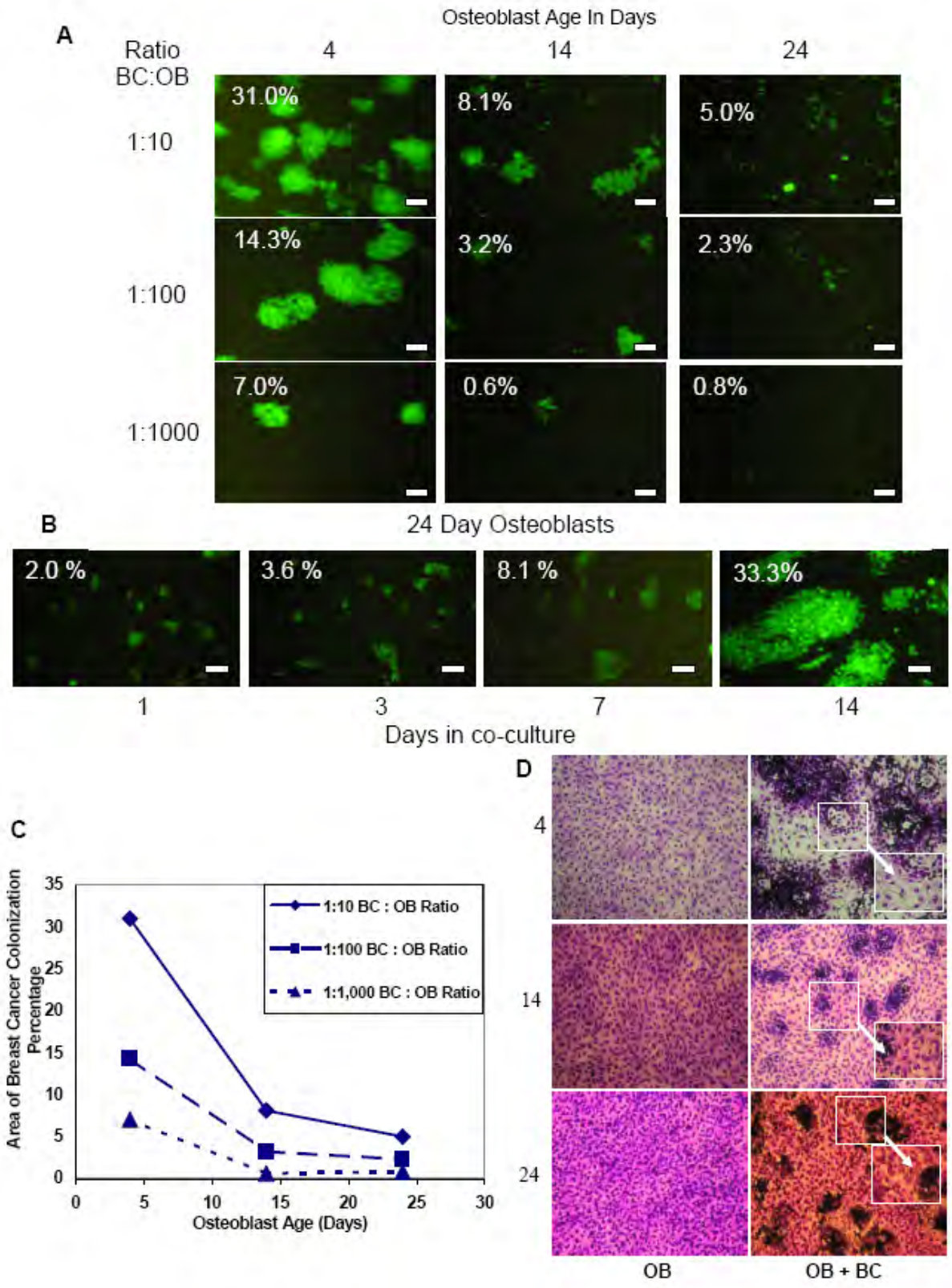
A
Osteoblast Age In Days
Ratio BC:OB
4
14
24
1:10
1:100
1:1000
31.0%
8.1%
5.0%
14.3%
3.2%
2.3%
7.0%
0.6%
0.8%
B
24 Day Osteoblasts
2.0 %
3.6 %
8.1 %
33.3%
1
3
7
14
Days in co-culture
C
Area of Breast Cancer Colonization Percentage
Osteoblast Age (Days)
1:10 BC : OB Ratio
1:100 BC : OB Ratio
1:1,000 BC : OB Ratio
D
4
14
24
OB
OB + BC

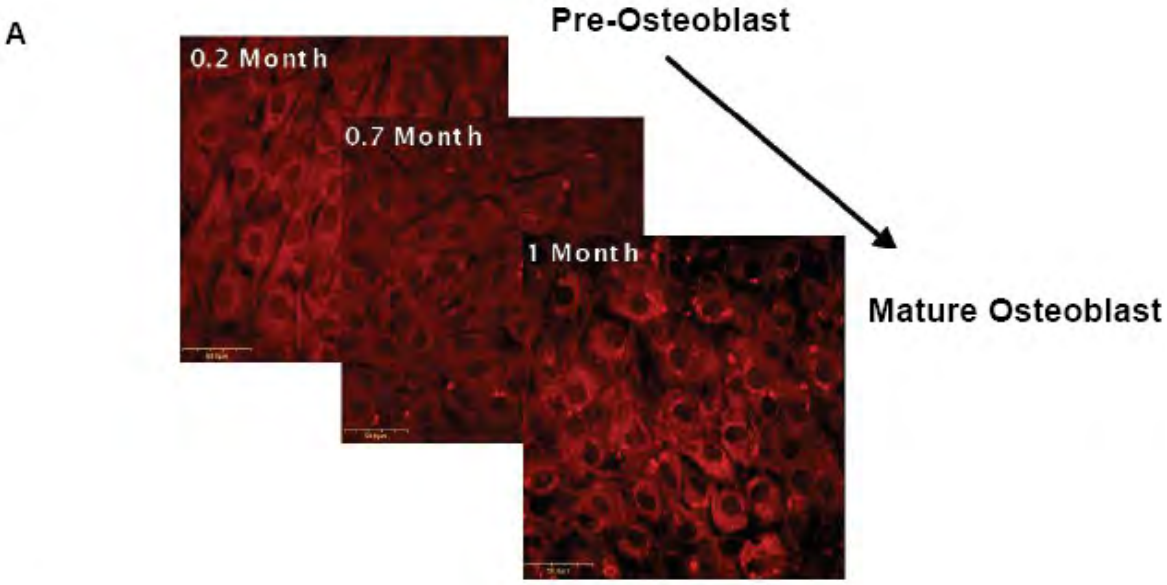
A
Pre-Osteoblast
0.2 Month
0.7 Month
1 Month
Mature Osteoblast

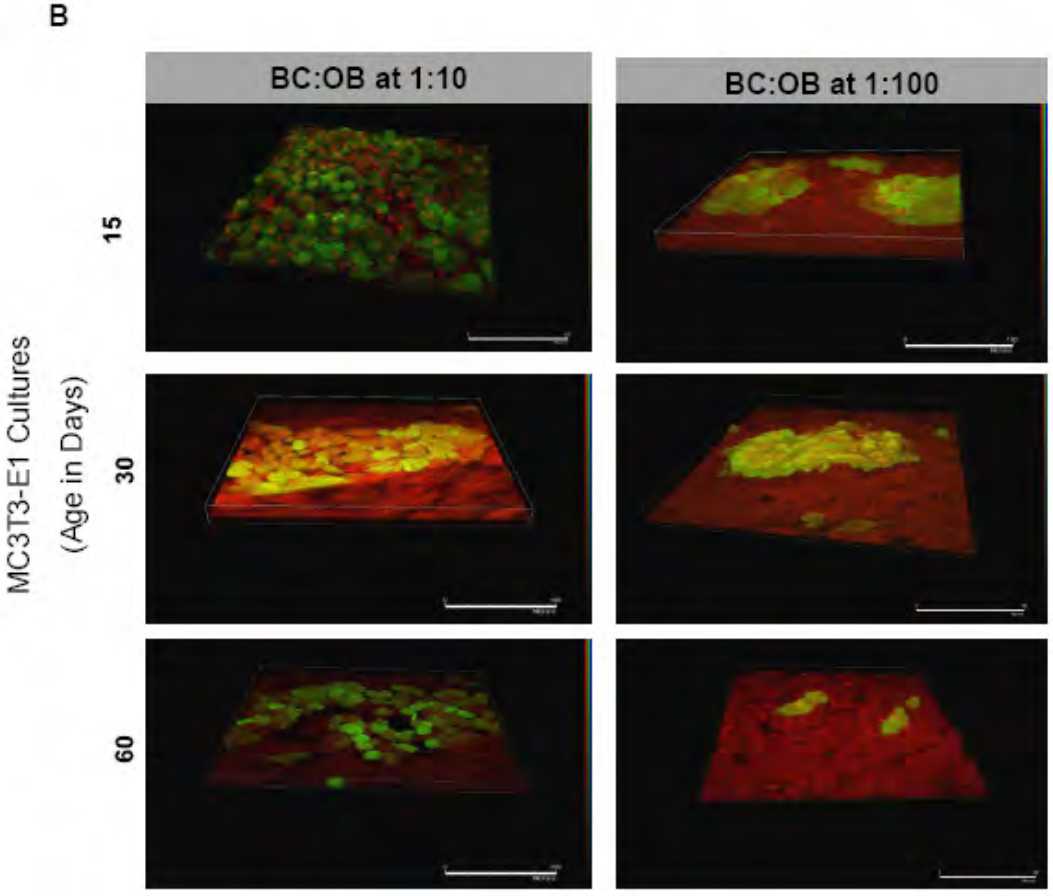
B
BC:OB at 1:10
BC:OB at 1:100
MC3T3-E1 Cultures
(Age in Days)
15
30
60

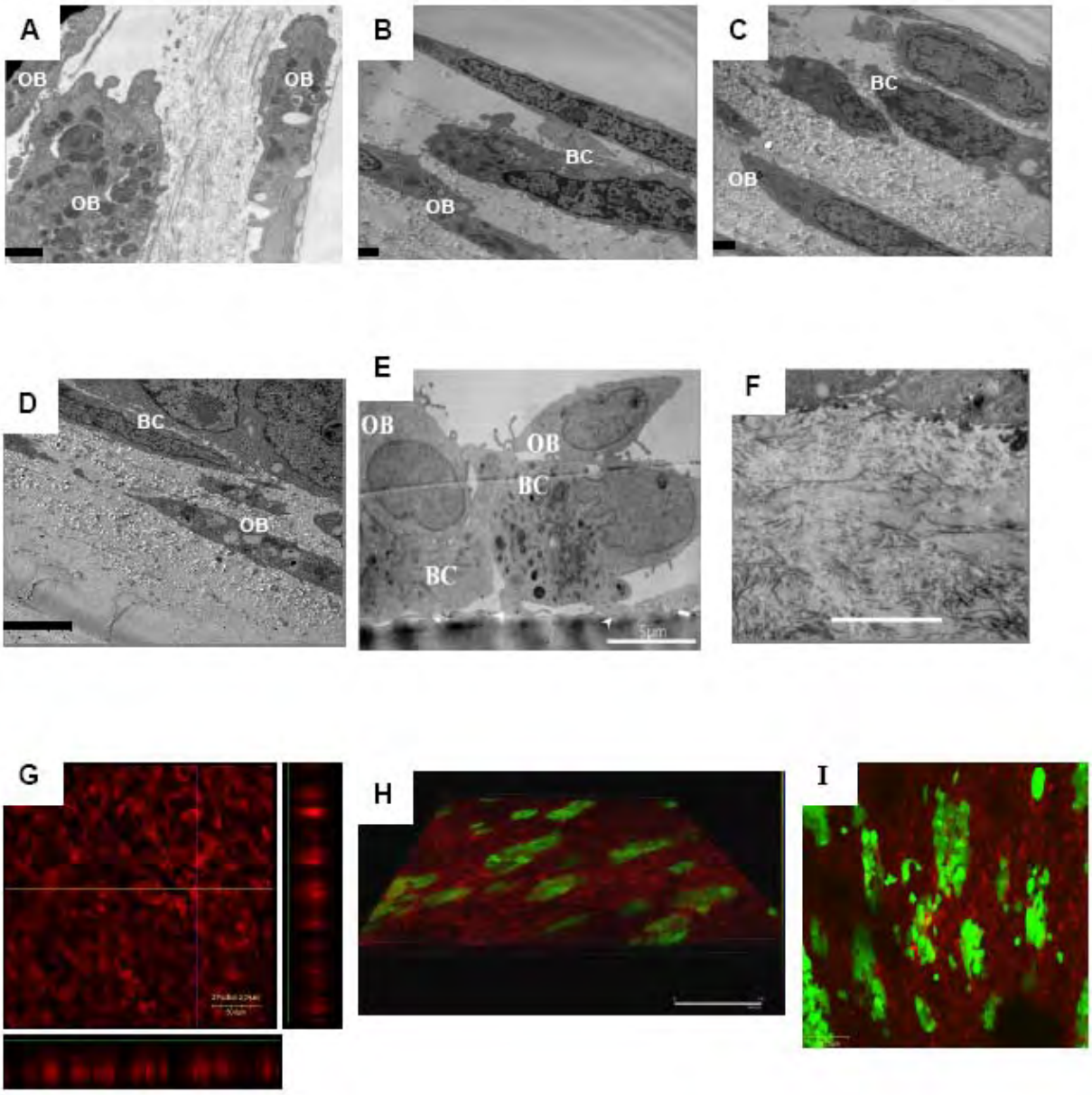
A
OB
OB
OB
B
BC
OB
C
BC
OB
D
BC
OB
E
OB
OB
BC
BC
F
G
H
I

A

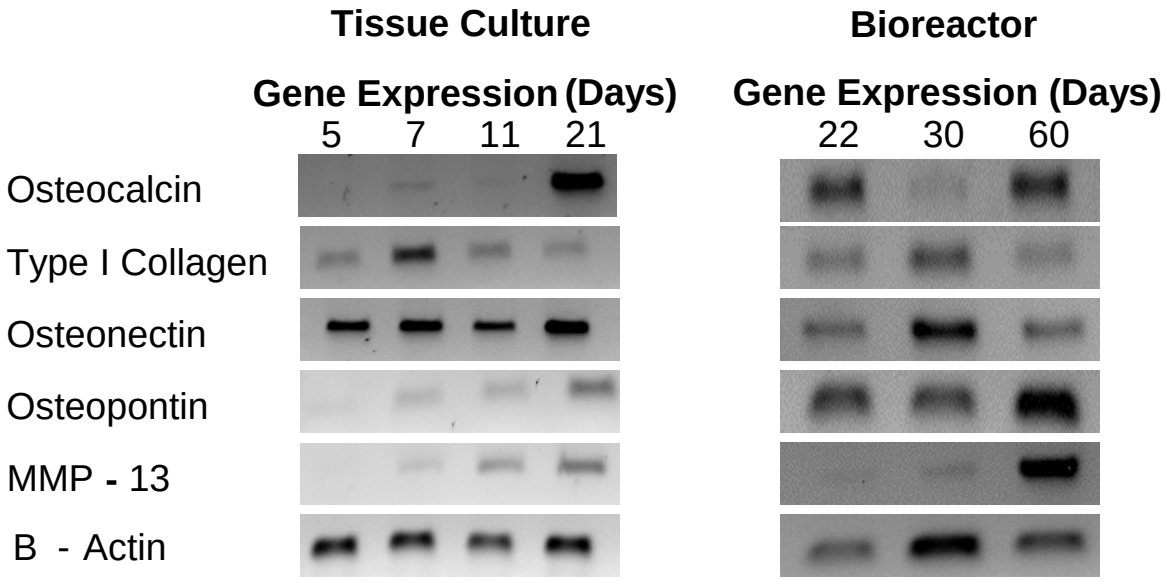
DIFFERENTIATION MARKERS
Tissue Culture
Bioreactor
Gene Expression (Days)
5 7 11 21
Gene Expression (Days)
22 30 60
Osteocalcin
Type I Collagen
Osteonectin
Osteopontin
MMP - 13
B - Actin

B

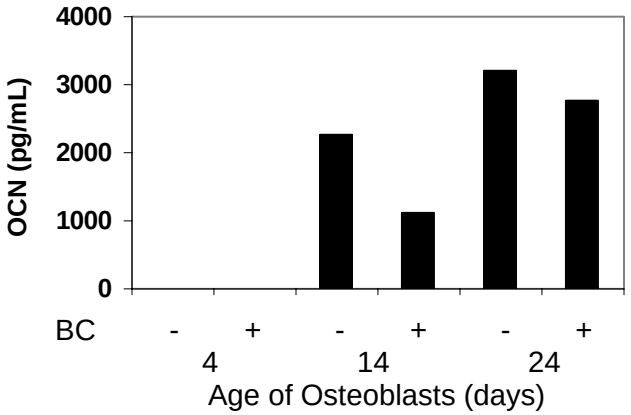
OCN (pg/mL)
4000
3000
2000
1000
0
BC - + - + - +
4 14 24
Age of Osteoblasts (days)

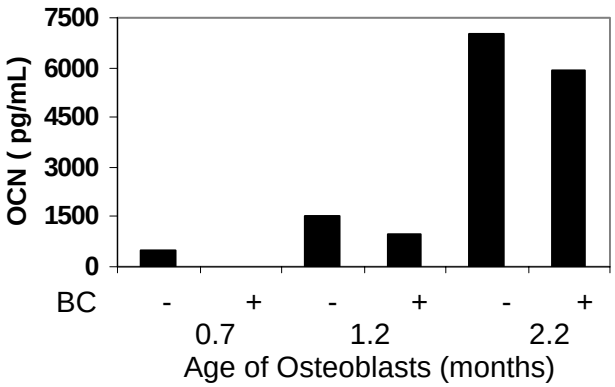
OCN (pg/mL)
7500
6000
4500
3000
1500
0
BC - + - + - +
0.7 1.2 2.2
Age of Osteoblasts (months)

C

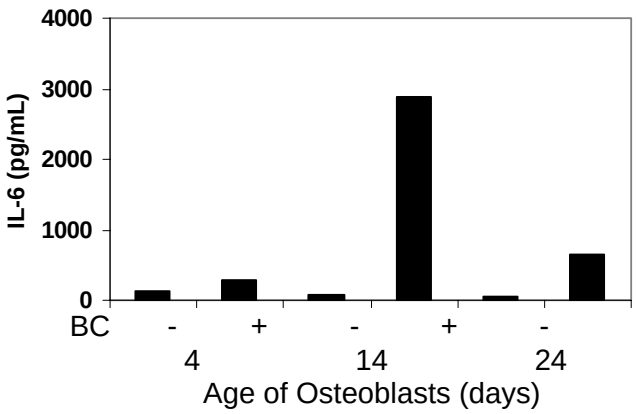
IL-6 (pg/mL)
4000
3000
2000
1000
0
BC - + - + -
4 14 24
Age of Osteoblasts (days)

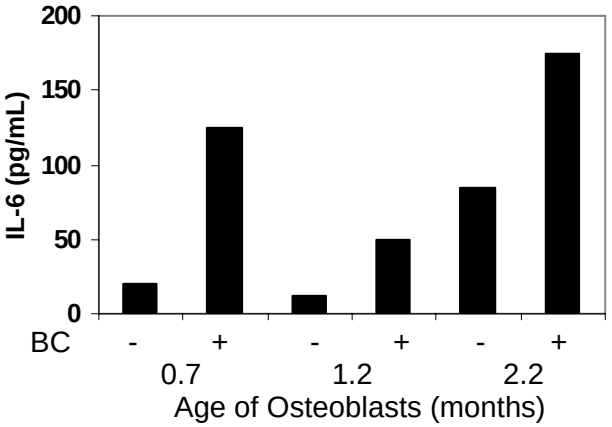
IL-6 (pg/mL)
200
150
100
50
0
BC - + - + - +
0.7 1.2 2.2
Age of Osteoblasts (months)